Numerical Simulation of Natural Convective Flow in an Inclined Cavity with Internal Heat Generation/ Absorption

By

Muhammad Yamin

MASTER OF PHILOSOPHY IN MATHEMATICS

DEPARTMENT OF MATHEMATICS
CAPITAL UNIVERSITY OF SCIENCE AND TECHNOLOGY
ISLAMABAD
2017

Numerical Simulation of Natural Convective Flow in an Inclined Cavity with Internal Heat Generation/ Absorption

By

Muhammad Yamin

A research thesis submitted to the Department of Mathematics,
Capital University of Science and Technology, Islamabad
in partial fulfillment of the requirements for the degree of

MASTER OF PHILOSOPHY IN MATHEMATICS

DEPARTMENT OF MATHEMATICS
CAPITAL UNIVERSITY OF SCIENCE AND TECHNOLOGY
ISLAMABAD
2017

CAPITAL UNIVERSITY OF SCIENCE & TECHNOLOGY
ISLAMABAD
Islamabad Expressway, Kahuta Road, Zone-V, Islamabad
Phone: +92 51 111 555 666, Fax: 92 51 4486705
Email: info@cust.edu.pk, Website: http"//www.cust.edu.pk

CERTIFICATE OF APPROVAL

Numerical Simulation of Natural Convective Flow in an Inclined Cavity with Internal Heat Generation/Absorption

by

Muhammad Yamin

MMT153004

THESIS EXAMINING COMMITTEE

S No	Examiner	Name	Organization
(a)	External Examiner	Dr. Muhammad Sabeel	IST, Islamabad
(b)	Internal Examiner	Dr. Muhammad Sagheer	CUST, Islamabad
(c)	Supervisor	Dr. Shafqat Hussain	CUST, Islamabad

_____

Dr. Shafqat Hussain
Thesis Supervisor
Sep, 2017

_____

Dr. Muhammad Sagheer
Head of Department
Department of Mathematics
Dated : Sep, 2017

_____

Dr. Muhammad Abdul Qadir
Dean
Faculty of Computing
Dated : Sep, 2017

Certificate

This is to certify that Mr. Muhammad Yamin has incorporated all observations, suggestions and comments made by the external evaluators as well as the internal examiners and thesis supervisor. The title of his Thesis is: Numerical Simulation of Natural Convective Flow in an Inclined Cavity with Internal Heat Generation/ Absorption.

Dr. Shafqat Hussain
(Thesis Supervisor)

"It's not that I'm so smart, It's just that I stay with problems longer."

Albert Einstein

Abstract

The objective of this work is to analyze the influence of internal heat generation or absorption parameter on two dimensional, steady and incompressible natural convective flow in a square tilted cavity. The cavity is assumed with adiabatic conditions on the top and bottom walls, heated on the left wall and cooled on the right wall. The governing equations for the heat exchange and fluid flow have been solved numerically by utilizing Galerkin weighted residual finite element method. Discretization of the governing equations is carried out with the help of finite element method. In particular, velocity and temperature fields are discretized by the biquadratic element Q_2 and for pressure ${P_1}^{disc}$ is utilized. The impact of physical parameters on the heat and fluid flow are discussed in terms of streamlines and isotherms and viewed by some useful plots. Effect of the physical parameters in specified ranges such as heat generation/absorption parameter ($q^* = -10, -5, 0$ and 5), Prandtl number ($Pr = 0.025$), Raleigh number ($Ra = 10^3$-10^5) and inclination angle ($\phi = 15^\circ$, 30°, 60° and 75°) on the fluid flow and heat transfer has been investigated. A significant effect in the heat transfer has been observed for the heat generation/absorption parameter. It is found that the average Nusselt number shows a decreasing behavior for the heat generation parameter ($q^* > 0$), while in the case of heat absorption ($q^* < 0$), the rate of heat transfer is enhanced.

Acknowledgements

In the name of **ALLAH**, who is the most merciful and beneficient, created the universe and blessed the mankind with intelligence and wisdom to explore it secrets. Countless respect and endurance for Prophet Muhammad (Peace be upon him), the fortune of knowledge, who took the humanity out of ignorance and shows the rights path.

I would like to express my gratitude and immeasurable respect to my thesis supervisor **Dr. Shafqat Hussain**, Associate Professor, Capital University of Science and Technology, Islamabad whose enthusiasm, willingness to help, and patience are limitless and I have benefited from these qualities during my thesis. His profound expertise in the research fields has been both an asset and a source of inspiration.

I am extremely grateful to my teacher **Dr. Muhammad Sagheer**, HoD Mathematics department, Capital University of science and technology, Islamabad for his continuing belief in my potential, for his encouraging and enthusiastic attitude and for many imparted words of wisdom. I would also like to thank my respectabe teachers **Dr. Rashid** and **Dr. Afzal** for their encouragement and emphasis on striving for excellence when teaching mathematics.

I offer my sincere gratitude to **Mr. Khalid Mehmod** for his productive guidance and continuing support during my thesis work. His kind and friendly behaviour has kept me motivated and encouraged.

My forever thanks goes to all research scholars, friends and colleagues in Mathematics lab for their friendship, help and providing a stimulating and encouraging environment. I wish to show my deep gratitude to my friends **Mr. Farrukh Saleem**, **Mr. Kamran Khan** and **Asifa Ashraf** for their love, personal interest and moral support.

At this juncture, I pay deep regards and thanks to my beloved parents, whose selfless care, love, devotion and prayers have made me able to achieve this goal. May Allah bless them all.

Muhammad Yamin

Contents

List of Figures

List of Tables

Abbreviations

PDEs	**P**artial **D**ifferential **E**quations
BVP	**B**oundary **V**alue **P**roblem
FEM	**F**inite **E**lement **M**ethod

Symbols

g	gravitational acceleration ($m\ s^{-2}$)
L	length of the square cavity
Nu	local Nusselt number
Nu_{avg}	average Nusselt number
p	pressure (Pa)
P	dimensionless pressure
Pr	Prandtl number ($\frac{\mu c_p}{k}$)
Ra	Raleigh number ($\frac{gB}{\nu\alpha}(T_h - T_c)L^3$)
q^*	dimensionless heat generation/absorption parameter
T	fluid temperature (K)
T_h	hot left wall temperature (k)
T_c	cold right wall temperature (k)
u	velocity in x-direction ($m\ s^{-1}$)
v	velocity in y-direction ($m\ s^{-1}$)
U	dimensionless velocity component in x-direction
V	dimensionless velocity component in y-direction
X	dimensionless x coordinate
Y	dimensionless y coordinate
Greek symbols	
α	thermal diffusivity (m^2s^{-1})
β	volume expansion coefficient (K^{-1})
θ	dimensionless temperature $(T - T_c)/\Delta T$
μ	dynamic viscosity($kg\ m^{-1}\ s^{-1}$)
ρ	density ($kg\ m^{-3}$)
ν	kinematic viscosity(m^2s^{-1})

ΔT	temperature gradient $T_h - T_c$
ϕ	angle of inclination
ψ	dimensionless stream function

Subscripts

c	cold
f	fluid
h	hot

This thesis is dedicated to my father, ***Muhammad Javed*** *who has always been a source of inspiration, encouragement and stamina to undertake my higher studies, to my loving* ***Mom*** *and to all my teachers, especially my thesis supervisor* ***Dr Shafqat Hussain****.*

Chapter 1

Introduction

Natural convection is a heat transport process caused by the buoyancy force in the fluid flow. The study of natural convective flow has been receiving a great attention in recent years based on various applications in many fields of engineering including cooling devices [1], thermoelastic damping [2], solar collectors [3], thermal flow in boiler tubes [4], rarefied gas flows [5], welding [6] etc. Due to this tremendous and widespread expansion of free convection applications, many researchers are incessantly investigating the convective heat flow in various physical systems such as magnetohydrodynamics convection [7–9], forced convection [10], convection of nanofluids [11–13] etc. However, convective flow within a square cavity is one of the most investigated solution of Navier-Stokes equations. This simple geometry of the problem has made its study much familiar among scientists.

Natural convective flow within the cavities is investigated by many researchers. A few earlier publications on the natural convection flow within enclosures with various boundary conditions are discussed here. Roy and Basak [14] numerically performed the simulations on natural convection flow in square enclosure heated at the bottom wall, the top wall being insulated and the vertical walls are at various hot/cold temperature. The convective heat transfer is observed both analytically and numerically in a square enclosure, filled with water heated from bottom and cooled along one vertical wall by November and Nasteel [15]. The significant enhancement in the heat transfer is obtained when bottom wall of the cavity is less than the half heated. Shiralker and Tein [16] investigated the simultaneous differential heating impact of the vertical walls as well as

the horizontal walls of the square enclosure. Numerical study of the free convection flow in a rectangular enclosure cooled on one side and heated from bottom is investigated by Ganzarolli and Milanez [17].

In past few years, particular attention has been given to examine the convective heat flow in enclosures with different geometries. Based on the observations it was established that the attributes of the fluid and heat flow are very sensitive to the geometry [18–22]. Many researchers have also paid a more important attention on the inclination angle effects on the thermal flow characteristics within inclined cavities [23, 24].

The studies on the heat flow characteristics in inclined cavities are examined by few researchers [23–34]. Biswal *et al.* [23] numerically inspected the impact of angle of inclination on free convection in tilted square cavity with porous media. They considered two cases corresponding to the bottom wall which is heated due to isothermal and non-isothermal heating. They concluded that non-isothermal heating, comparatively to the isothermal heating, in heating strategy is efficient with realistic thermal management. The detailed analysis of convective heat transfer inside square tilted cavities with oppositely cooled vertical walls and insulated top wall is parallel to the bottom hot wall were discussed by Singh *et al.* [24]. In 2004, Cianfrini *et al.* [25] investigated the influence of angle of inclination on heat transport in square enclosure with opposite walls are differentially heated. They obtained the significant effect of the angle of inclination on overall heat transport in both x-direction and y-direction which is comparatively larger than that of untilted case. The study of free convection heat flow inside a rectangular cavity with porous media for various values of inclination angle is investigated numerically by Baez and Nicolas [26].

Dalal and Das [27] presented convective heat flow in a tilted cavity subjected to a sinusoidal temperature on one wall and other walls are kept at constant temperature. Their results have shown that the flow and rate of heat transfer is enhanced by inclination angle. Natural convection flow and characteristics of heat transfer within L-shaped inclined enclosure was studied by Tasnim and Mahmud [28]. In 2008, Jeng *et al.* [29] have performed study on transient natural convective flow and mass transfer both numerically and experimentally in inclined enclosures for different inclination angles. It was observed from the results that the inclination angle has a substantial effect on the

entire flow.

Ozoe *et al.* [30] analyzed the rate of heat transfer experimentally as well as numerically within an inclined cavity in which the inclined side is kept at constant hot temperature while the opposite side is provided with low temperature. Rasoul and Prinos [31] analyzed numerically the influence of inclined cavity on laminar natural convection for various Prandtl numbers and Raleigh numbers. It was noticed that increase in inclination angle resulting into decrease in average Nusselt number, irrespective of Prandtl number and Raleigh numbers. More comprehensive study on natural convection with the effect of inclination angle is also examined by Cotton *et al.* [32], Hamady *et al.* [33] and Al-Farhany and Turan [34] for various parameters and arbitrary inclination angles.

Natural convection driven by heat generation/absorption involve in large number of physical phenomena. In moving fluids, the significance of the heat generation has been noticed in various problems concerning with chemical reaction and dissociating fluids. The influence of internal heat generation may alter the distribution of temperature and therefore, the particle deposition rate. Moreover, the investigation of internal heat generation effects are much important in number of applications including metal waste, food stuffs storage and reactor safety analysis. The study of natural convection with internat heat generation in various geometries has been investigated by several investigators [35–37] and, motivated by these works; the current project is intended to analyze the impact of heat generation/absorption on steady and incompressible natural convection flow in a tilted square cavity.

1.1 Thesis contributions

Aim of this study is to investigate the natural convection heat flow with internal heat generation/absorption parameter inside an inclined square cavity. The Galerkin weighted residual method is adopted to solve the equations governing the heat exchange and fluid flow. Finite element Q_2 is used to discretize the velocity and temperature, and discontinuous P_1 element is for the pressure. The numerical results of the problem are plotted and analyzed in terms of isotherms and streamlines. Effect of the physical parameters in

specified ranges such as heat generation/absorption parameter, Prandtl number, Raleigh number and inclination angle on the flow and heat transfer have also been investigated.

1.2 Thesis layout

This dissertation further comprises of four chapters.

- **Chapter 2** contains some basic definitions and physical laws regarding this work. Also, the numerical method used for the simulation of the concerned problem is explained stepwise and illustrated by an example.
- **Chapter 3** targets the review of the research paper Basak *et al.* [38]. In this chapter, the steady natural convective flow is inspected in square cavity inclined at different angles. A suitable transformation is used to convert equations governing the flow into non-dimensional form and solve these nonlinear coupled PDEs numerically using Galerkin finite element method. Numerical results are calculated for various parameters such as Pr, Ra and inclination angle ϕ.
- In **Chapter 4** the work of Basak *et al.* [38] is extended with the idea of internal heat generation/absorption. The non-dimensional governing equations are discretized using biquadratic element Q_2 for velocity and temperature, and discontinuous P_1 element for pressure. Simulations are performed for various parameters such as heat generation/absorption q^*, Pr, Ra and ϕ, and their corresponding effects can be seen through streamlines and isotherms.
- Finally in **Chapter 5** results of the current thesis are concluded.

Chapter 2

Some basic definitions and governing equations

2.1 Basic definitions

This chapter contains some basic definitions of fluid flow and its properties, heat transfer, dimensionless numbers and physical laws regarding this work [39]. The procedure of finite element method is also explained and illustrated by a two dimensional Poisson problem.

Definition 2.1.1. (Fluid)
A matter which continuously changes its shape under the influence of shear stress is called fluid. It yields easily to shear stress and repeatedly deforms its shape as long as the shear stress acts. Fluid has no fixed shape and conforms to the shape of a container in which it is placed.

Definition 2.1.2. (Fluid mechanics)
The study of fluid mechanics is concerned with various properties of fluid and the forces acting on them. Fluid mechanics is mainly divided into two categories: fluid static which deals with the study of fluid at rest and fluid dynamic which deals with the study of fluid in motion.

Definition 2.1.3. (Pressure)

An expression of applied force to the unit area is said to be pressure. It is denoted by P and mathematically, it can be written as

$$P = \frac{F}{A}, \tag{2.1}$$

where F, A denote the applied force and area of the surface, respectively.

Definition 2.1.4. (Density)

Mass of an object per unit its volume is called density of that object. The most often symbol used for it is ρ and mathematically written as

$$\rho = \frac{m}{\mathbf{V}}, \tag{2.2}$$

The terms $\mathbf{V}$ and m in the above expression are the volume of the material and mass of the material, respectively.

Definition 2.1.5. (Stress)

Stress is a force acted upon a material per unit of its area and is denoted by σ. Mathematically, it can be written as;

$$\tau = \frac{F}{A}, \tag{2.3}$$

where F denotes the force and A represents area.

Definition 2.1.6. (Shear stress)

It is a type of stress in which the force vector acts parallel to the material surface or cross section of a material.

Definition 2.1.7. (Normal stress)

Normal stress is a type of stress in which force vector acts perpendicular to the surface of the material or cross section of a material.

Definition 2.1.8. (Yield stress)

It is the property of a material at which it begins to deform plastically.

Definition 2.1.9. (Viscosity)

Viscosity of a fluid is defined as the measure of resistance to steady distortion by shear/tensile stress. A notation used for viscosity is μ and its mathematical expression is

$$\text{viscosity}(\mu) = \frac{\text{shear stress}}{\text{shear strain}}. \tag{2.4}$$

Definition 2.1.10. (Kinematic viscosity)

The relationship between dynamic viscosity to the fluid density is called kinematic viscosity. It is denoted by symbol ν and can be expressed mathematically as

$$\nu = \frac{\mu}{\rho}, \tag{2.5}$$

where μ and ρ denote the dynamic viscosity and the density respectively.

2.2 Classification of fluids

Definition 2.2.1. (Ideal fluid)

An incompressible fluid having zero viscosity is said to be an ideal or inviscid fluid. Shear stress has no existence in an deal fluid as the viscosity of it is zero.

Definition 2.2.2. (Real fluid)

A compressible fluid which experience some resistance during the flow is characterized as a real or viscid fluid.

Definition 2.2.3. (Newton's law of viscosity)

It is a relationship in which shear stress is directly and linearly proportional to the velocity gradient. Mathematically, it can be written as

$$\tau_{yx} \propto \left(\frac{du}{dy}\right),$$

$$\tau_{yx} = \mu \left(\frac{du}{dy} \right). \tag{2.6}$$

In the above expression, τ_{yx} is the shear stress applied to the velocity component u of fluid and μ is the viscosity proportionality constant.

Definition 2.2.4. (Newtonian fluid)

Those fluids are categorized as Netownian, for which the shear stress varies directly and linearly as the deformation rate. Shear stress of Newtonian fluid is mathematically defined as

$$\tau_{yx} = \mu \left(\frac{du}{dy} \right), \tag{2.7}$$

where τ_{yx} is the shear stress, u denotes the x-component of velocity and μ the dynamic viscosity. Examples of Newtonian fluids are air, water, oxygen gas and silicone oil etc.

Definition 2.2.5. (Non-Newtonian fluid)

For non-Newtonian fluid, the relationship between shear stress is and the deformation rate is not linear. It can also be defined as, the fluid which does not satisfy the Newton's law of viscosity is called Non-Newtonian fluids. Mathematically, it can be written as

$$\tau_{yx} \propto \left(\frac{du}{dy} \right)^m, \ m \neq 1$$

$$\tau_{yx} = \mu \left(\frac{du}{dy} \right)^m. \tag{2.8}$$

Here μ denotes the viscosity and m the index of the flow performance. Some common examples of non-Newtonian fluids are shampoo, grease, paint, blood and melt polymer etc.

2.3 Flows

Definition 2.3.1. (Flow)

An object exhibits the flow if unbalanced forces lead to a limitless deformation.

Definition 2.3.2. (Laminar flow)

The flow in which fluid particles move very orderly and in parallel layers is said to be

laminar. The example of laminar flow is the rising of cigarette smoke. If we observe the smoke rising for the first few seconds the flow seems to be laminar but later it becomes turbulent.

Definition 2.3.3. (Uniform flow)

A flow, where the velocity of each fluid particle remains unchanged at any instant of time is called uniform flow. Mathematically, it can be written as

$$\frac{dV}{ds} = 0, \tag{2.9}$$

where V is the velocity and s is the displacement in any direction.

Definition 2.3.4. (Non uniform flow)

A flow in which the velocity of fluid particles varies from point to point at a given instant of time is known as uniform flow. Mathematically, it is expressed as

$$\frac{dV}{ds} \neq 0, \tag{2.10}$$

where V is the velocity and s is the displacement.

Definition 2.3.5. (Internal flow)

Fluid flow which is bounded by the solid surface is known as internal flow. The flow in a pipe is an example of the internal flow.

Definition 2.3.6. (External flow)

The flow which is not confined by the solid surface, is known as external flow. The flow of water in the ocean or in the river is an example of the external flow.

Definition 2.3.7. (Steady flow)

A flow in which properties of the fluid have no dependency on time is said to be steady flow. Mathematically, it can be written as

$$\frac{d\xi}{dt} = 0, \tag{2.11}$$

where ξ is fluid property.

Definition 2.3.8. (Unsteady flow)

A fluid flow in which fluid properties are dependent of time is known as unsteady flow. Mathematically, it can be written as

$$\frac{d\xi}{dt} \neq 0, \tag{2.12}$$

where ξ is fluid property.

Definition 2.3.9. (Compressible flow)

Fluid flow which has varying density with respect to the substance variable is said to be compressible flow. Mathematically, it is expressed by

$$\rho(x, y, z, t) \neq c, \quad c \; is \; a \text{ constant}. \tag{2.13}$$

Definition 2.3.10. (Incompressible flow)

Flow of a fluid is said to be incompressible when the material density during the flow remains constant. It can be expressed mathematically as

$$\rho(x, y, z, t) = c, \tag{2.14}$$

where c is a constant.

2.4 Some basic definitions of heat transfer

Definition 2.4.1. (Conduction)

In conduction process, the transmission of heat through matter occurs by the intersection of free electrons and molecules. In other words, when heat is transferred from one object to another due to the molecular interaction without disturbance or motion of the material as whole then the process is known as conduction. Mathematically, it can be written as

$$q = -kA\left(\frac{\Delta T}{\Delta n}\right), \tag{2.15}$$

where k and $\frac{\Delta T}{\Delta n}$ denote the constant of the thermal conductivity and gradient of the temperature respectively.

Definition 2.4.2. (Convection)

It is a mechanism in which heat transfer occurs due to the motion of molecules within the fluid such as air and water. The convection phenomenon takes place through diffusion or advection. A mathematical expression for convection phenomena is

$$q = hA(T_s - T_\infty), \tag{2.16}$$

where h, A, T_s and T_∞ denote the heat transfer coefficient, the area, the temperature of the surface and the temperature away from the surface respectively. Further, it is subdivided into the following three categories.

Forced convection

It is a type of heat transfer in which an external source is used to produce motion of the fluid. e.g. fan or a pump.

Natural convection

In a process of heat transfer where motion of the fluid particles is not generated by an independent source, but occurs naturally is called natural convection or free convection. It occurs in a fluid only when there is a density difference.

Mixed convection

A convection mechanism in which heat is transferred by the combination of both forced and natural convection process, is called mixed convection.

Definition 2.4.3. (Radiation)

In radiation process, heat is transferred through electromagnetic waves or rays. An example of radiation would be atmosphere, the atmosphere is heated by the radiation of the sun. Mathematically, it can be written as

$$q = E\sigma^* A[(\Delta T)^4], \tag{2.17}$$

where E, σ^*, $(\Delta T)^4$, A, q are the emissivity of the scheme, the constant of Stephan-Boltzmann ($5.670 \times 10^{-}8\frac{W}{m^2K^4}$), the variation of the temperature, the area and the heat transfer respectively.

2.5 Thermal conductivity

It is the property of a substance which measures the ability to transfer heat. Fourier's law of conduction which relates the flow rate of heat by conduction to the temperature gradient is

$$\frac{dQ}{dt} = -kA\frac{dT}{dx}, \tag{2.18}$$

where A, k, $\frac{dT}{dx}$, $\frac{dQ}{dt}$ are the area, the thermal conductivity, the temperature and the rate of heat transfer, respectively. The SI unit of thermal conductivity is $\frac{Kg.m}{s^3}$ and the dimension of thermal conductivity is $[\frac{ML}{T^3}]$.

2.6 Thermal diffusivity

The ratio of the unsteady heat conduction (k) of a substance to the product of specific heat capacity (c_p) and density (ρ) is called thermal diffusivity. It quantify the ability of a substance to transfer heat rather to store it. Mathematically, it can be written as

$$\alpha = \frac{k}{\rho c_p}, \tag{2.19}$$

2.7 Dimensionless numbers

Definition 2.7.1. (Prandtl number)
The ratio of kinematic diffusivity to the heat diffusivity is said to be Prandtl number. It is denoted by Pr and mathematically it can be written as

$$Pr = \frac{\nu}{\alpha},$$

$$Pr = \frac{\frac{\mu}{\rho}}{\frac{k}{\rho c_p}},$$

$$Pr = \frac{\mu c_p}{k}. \tag{2.20}$$

where ν and α denote the momentum diffusivity or kinematic diffusivity and the thermal diffusivity respectively. Physical importance of Prandtl number is that it provides the respective thickness of thermal boundary layer and velocity boundary layer. Heat distributes rapidly relative to the momentum for small values of Pr.

Definition 2.7.2. (Raleigh number)

It is the relationship between the kinematic diffusivity to heat diffusivity multiplied by the ratio of viscosity forces and buoyancy forces. It is a dimensionless number introduced by Lord Raleigh. It is denoted by Ra and mathematically it can be written as

$$Ra = \frac{g\beta}{\nu\alpha}(T_h - T_c)L^3, \tag{2.21}$$

Definition 2.7.3. (Nusselt number)

It is the relationship between the convective to the conductive heat transfer through the boundary of the surface. It is a dimensionless number which was first introduced by the German mathematician Nusselt. Heat transfer due to conduction is denoted by $\frac{k\Delta T}{\delta}$ and heat transfer due to convection is denoted by $h\Delta T$. It is denoted by Nu and mathematically, it is expressed by

$$Nu = \frac{h\Delta T}{\frac{k\Delta T}{\delta}},$$

$$Nu = \frac{h\delta}{k}, \tag{2.22}$$

where h, δ, k denote the coefficient of heat transfer, the characteristic length and the thermal conductivity respectively.

2.8 Basic equations

Definition 2.8.1. (Continuity equation)

The equation of continuity is derived from the mass conservation law and mathematically, it is expressed by

$$\frac{\partial \rho}{\partial t} + \nabla.(\rho V) = 0, \tag{2.23}$$

where t is the time. If fluid is an incompressible, then the continuity equation is expressed by

$$\nabla.V = 0. \tag{2.24}$$

Definition 2.8.2. (Law of conservation of momentum)

Each particle of fluid obeys Newton's second law of motion which is at rest or in steady state or accelerated motion. This law states that the combination of all applied external forces working on an object is equal to the time rate of change of its linear momentum. In vector notation this law is expressed as

$$\rho \frac{dV}{dt} = \text{div } \tau + \rho b, \tag{2.25}$$

For Navier-Stokes equation

$$\tau = -pI + \mu A_1, \tag{2.26}$$

where A_1 is the tensor and first time it was produced by Rivlin-Erickson.

$$A_1 = \text{grad } V + (\text{grad } V)^t, \tag{2.27}$$

In the above equations, $\frac{d}{dt}$ denote the material time derivative or total derivative, V denote velocity field, ρ denote density, τ here denotes the Cauchy stress tensor, b the body forces, p is the pressure and μ the dynamic viscosity.

The stress tensor τ is expressed in the matrix form as

$$\tau = \begin{pmatrix} \sigma_{xx} & \tau_{yx} & \tau_{zx} \\ \tau_{xy} & \sigma_{yy} & \tau_{zy} \\ \tau_{xz} & \tau_{yz} & \sigma_{zz} \end{pmatrix}, \tag{2.28}$$

where σ_{xx}, σ_{yy} and σ_{zz} are normal stresses, others wise the shear stresses. For two-dimensional flow, we have $V = [u(x, y, 0), v(x, y, 0), 0]$ and thus

$$\text{grad } V = \begin{pmatrix} \frac{\partial u}{\partial x} & \frac{\partial u}{\partial y} & 0 \\ \frac{\partial v}{\partial x} & \frac{\partial v}{\partial y} & 0 \\ 0 & 0 & 0 \end{pmatrix}, \tag{2.29}$$

$$\frac{\partial u}{\partial t} + u\frac{\partial u}{\partial x} + v\frac{\partial u}{\partial y} = -\frac{1}{\rho}\frac{\partial p}{\partial x} + \nu\left(\frac{\partial^2 u}{\partial x^2} + \frac{\partial^2 u}{\partial y^2}\right), \tag{2.30}$$

Similarly, we repeat the above process for Y component as follows:

$$\frac{\partial v}{\partial t} + u\frac{\partial v}{\partial x} + v\frac{\partial v}{\partial y} = -\frac{1}{\rho}\frac{\partial p}{\partial y} + \nu\left(\frac{\partial^2 v}{\partial x^2} + \frac{\partial^2 v}{\partial y^2}\right), \tag{2.31}$$

Definition 2.8.3. (Energy equation)

The energy equation for the fluid is

$$\rho c_p\left(\frac{\partial}{\partial t} + V\nabla\right)T = k\nabla^2 T + \tau L + \rho c_p\left[D_B \nabla C.\nabla T + \frac{DT}{T_m}\nabla T\right], \tag{2.32}$$

where $(c_p)_f$ denotes the specific heat of the basic fluid, $(c_p)_s$ the specific heat of the material, ρ_f the density of basic fluid, T is fluid temperature, L represent strain tensor rate, D_B denote the Brownian motion coefficient, DT the temperature diffusion coefficient and T_m denote the mean temperature. The expression for stress tensor τ for the incompressible fluid is expressed by

$$\tau = -pI + \mu A_1, \tag{2.33}$$

where A_1 is the tensor, p the pressure and μ the dynamic viscosity.

$$A_1 = \text{grad } V + (\text{grad } V)^t, \tag{2.34}$$

where t represents transpose of the matrix for two dimensional field velocity of the fluid, τ is the stess tensor and can be written as

$$\tau = \begin{pmatrix} \sigma_{xx} & \tau_{yx} & \tau_{zx} \\ \tau_{xy} & \sigma_{yy} & \tau_{zy} \\ \tau_{xz} & \tau_{yz} & \sigma_{zz} \end{pmatrix}. \tag{2.35}$$

2.9 Finite Element Method

Finite element was first introduced by Clough and is considered as a powerful computer oriented technique. It is a technique for approximating the solution to the problems of physics and engineering. Finite element method subdivides a huge problem into smaller parts, called as finite elements. The basic idea regarding FEM is to transform the governing equations into an appropriate form which is known as weak or variational form. In weak formulation the governing equations are multiplied by some suitable functions called the weight functions or test functions and then integrated over the whole domain. Examples of the weak formulation are the well known weighted residual method, the discontinuous Galerkin method, mixed method, etc. [40]

Definition 2.9.1. (Galerkin weighted residual method)
Among the finite element methods, Galerkin method of weighted residual is the most common method for calculating the global stiffness matrix. To solve the problems by using the finite element method, we carry out the following process.

1. Multiply both sides of governing equation of the problem by the test function $w(x) \in W$, that is vanishing on the boundaries of the domain, where W is a test space.

2. Perform integration by parts such that some derivative will be transferred from trial function to the test function.

3. Impose natural boundary conditions in the boundary integrals and essential boundary conditions to the trial and test spaces. This is called the variational formulation or weak formulation.

4. Generate mesh or triangulation:
   Divide the entire domain into non over-lapping elements. In one dimension, mesh is a set of points that is,
   $x_0 = 0, x_1, x_2, ..., x_N = 1$,
   where x_i is a node and $e_i = [x_i, x_{i+1}]$, is an element such that $e_i \bigcap e_j = \Phi$ for $i \neq j$.
   Let $h_i = x_i - x_{i-1}$ for $i = 0, 1, 2, 3, ..., N$. h_i is known as the mesh size.

5. Approximate the infinite dimensional trial space V and test spaces W by the finite dimensional spaces V_h and W_h respectively

$$V_h \text{ (finite dimensional space)} \subset V \text{ (the solution space)}.$$

To illustrate the method of Galerkin weighted residual, we consider the following example.

Example

- Consider a 2D Poisson problem

$$-\Delta u = f, \quad \text{in } \Omega \tag{2.36}$$

$$u = 0, \quad \text{on } \partial\Omega \tag{2.37}$$

where f is known function and u is to find, Ω is domain of the problem which is open, bounded and connected and $\partial\Omega$ is the boundary.

The Variational Form:

- The exact solution u of the Eq. (2.36) should be twice continuously differentiable and satisfying Eq. (2.36). Let w be a test function such that $w(x) = 0$ on the boundary of the domain.

- Weighted residual integral statement of the poisson problem (2.36) is

$$-\int_\Omega w\ \Delta u\ d\Omega = \int_\Omega wf\ d\Omega, \tag{2.38}$$

- 2^{nd} order derivatives of u can be reduced to 1^{st} order by using Green's formula.

$$\int_{\partial\Omega} w\frac{\partial u}{\partial n}\ ds = \int_\Omega \nabla w \nabla u\ d\Omega + \int_\Omega w\Delta u\ d\Omega, \tag{2.39}$$

- Using Eq. (2.39) in Eq. (2.38), we obtain

$$-\underbrace{\int_{\partial\Omega} w\frac{\partial u}{\partial n}\ ds}_{0} + \int_\Omega \nabla w \nabla u\ d\Omega = \int_\Omega wf\ d\Omega, \tag{2.40}$$

where the boundary integral vanishes due to the homogeneous boundary conditions, so we are left with

$$\int_{\Omega} \nabla w \nabla u \; d\Omega = \int_{\Omega} wf \; d\Omega, \tag{2.41}$$

- Elemental weak form is

$$\int_{\Omega^e} \nabla w \nabla u \; d\Omega = \int_{\Omega^e} wf \; d\Omega, \tag{2.42}$$

- In xy plane, Eq. (2.42) can be written as

$$\int_{\Omega^e} \left(\frac{\partial w}{\partial x} \frac{\partial u}{\partial x} + \frac{\partial w}{\partial y} \frac{\partial u}{\partial y} \right) \; d\Omega = \int_{\Omega^e} wf \; d\Omega, \tag{2.43}$$

- Approximate solution over an element is

$$u^e = \sum_{i=1}^{NEN} {u_j}^e {S_j}^e(x, y). \tag{2.44}$$

where S_j is a shape function and u_j are the solution values at nodes.

2.9.1 Advantages of FEM

- Finite element method is useful for managing complicated geometrical boundaries [40].
- FEM can handle a wide variety of engineering problems [41].
- There are many commercial packages based on finite element method. i.e., ADINA, ANSYS for analyzing pratical problems.

Chapter 3

Simulations of natural convective flow in an inclined square cavity

In this chapter, we numerically find the solution for the steady and incompressible natural convective flow in a square tilted cavity. By means of an appropriate transformation, the governing equations are transformed into dimensionless coupled partial differential equations. These dimensionless governing equations has been solved by employing the finite element technique together with Galerkin weighed residual method. The influence of governing parameters is analyzed through streamlines and isotherms. In this chapter, a review of the article [38] is presented.

3.1 Problem Description and Mathematical Formulation

Let us take a two-dimensional, steady and incompressible natural convective flow in a tilted square cavity. The schematic diagram of the problem under consideration with boundary conditions is shown in Figure 3.1. The cavity is tilted at an inclination angle ϕ° with horizontal coordinate. Two parallel walls AB and CD of the cavity are assumed to be adiabatic where the wall BC is kept cold at temperature T_c (cold wall) and the wall DA of the cavity is maintained at high temperature T_h (hot wall). By means of Boussinesq approximation, a change in density which arises due to variation in the fluid temperature is calculated while other physical properties of the density differences are

ignored except in the buoyancy term. Navier-stokes equation and energy equation governing the flow inside the cavity have been given below.

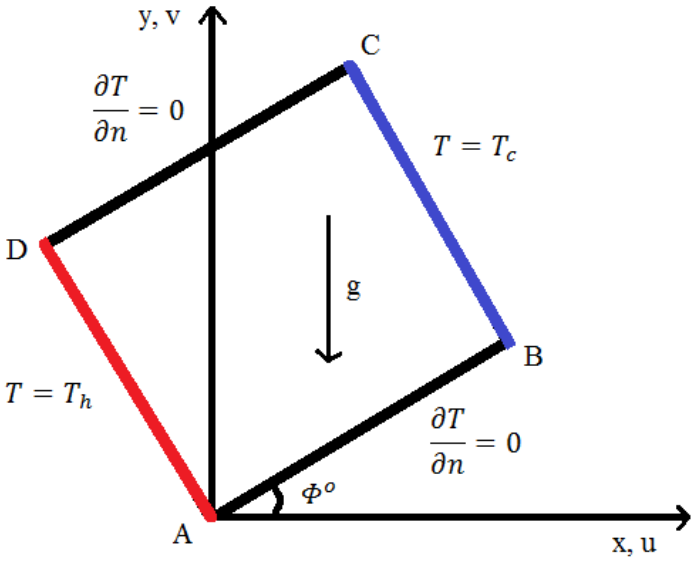

FIGURE 3.1: Geometry of the problem.

Continuity equation:

$$\frac{\partial u}{\partial x} + \frac{\partial v}{\partial y} = 0, \tag{3.1}$$

x-momentum equation:

$$u\frac{\partial u}{\partial x} + v\frac{\partial u}{\partial y} = -\frac{1}{\rho}\frac{\partial p}{\partial x} + \nu\left(\frac{\partial^2 u}{\partial x^2} + \frac{\partial^2 u}{\partial y^2}\right) + g\beta(T - T_c)\sin\phi, \tag{3.2}$$

y-momentum equation:

$$u\frac{\partial v}{\partial x} + v\frac{\partial v}{\partial y} = -\frac{1}{\rho}\frac{\partial p}{\partial y} + \nu\left(\frac{\partial^2 v}{\partial x^2} + \frac{\partial^2 v}{\partial y^2}\right) + g\beta(T - T_c)\cos\phi, \tag{3.3}$$

Energy equation:

$$u\frac{\partial T}{\partial x} + v\frac{\partial T}{\partial y} = \alpha\left(\frac{\partial^2 T}{\partial x^2} + \frac{\partial^2 T}{\partial y^2}\right). \tag{3.4}$$

Here ν represent the kinematic fluid viscosity, ρ is fluid density, α is the thermal diffusivity, the expansion coefficient is β, ϕ is an inclination angle, fluid temperature is T, T_c is the cold right wall temperature, acceleration due to gravity is g, p is pressure of the

fluid and u, v denote the components of velocity.

The dimensional boundary conditions on each wall of the cavity for velocity and temperature fields are given by

- On the horizontal walls AB and CD:

$$u(x,y) = 0, \quad v(x,y) = 0, \quad \frac{\partial T}{\partial n} = 0 \tag{3.5}$$

- On the right wall BC:

$$u(x,y) = 0, \quad v(x,y) = 0, \quad T = T_c \tag{3.6}$$

- On the left Wall DA:

$$u(x,y) = 0, \quad v(x,y) = 0, \quad T = T_h \tag{3.7}$$

where n denotes the normal vector.

3.1.1 Dimensionless Form of the Governing Equations

The dimensionless form of the Eqs. (3.1)-(3.4) may be obtained by using the following dimensionless parameters [38].

$$X = \frac{x}{L}, \qquad Y = \frac{y}{L}, \qquad U = \frac{uL}{\alpha}, \qquad V = \frac{vL}{\alpha}, \qquad P = \frac{pL^2}{\rho\alpha^2}, \qquad \theta = \frac{T-T_c}{T_h-T_c}$$

$$Pr = \frac{\nu}{\alpha}, \qquad Ra = \frac{g\beta(T_h-T_c)L^3Pr}{\nu^2}.$$

The above parameters leads to the following dimensionless governing equations.

$$\frac{\partial U}{\partial X} + \frac{\partial V}{\partial Y} = 0, \tag{3.8}$$

$$U\frac{\partial U}{\partial X} + V\frac{\partial U}{\partial Y} = -\frac{\partial P}{\partial X} + Pr\left(\frac{\partial^2 U}{\partial X^2} + \frac{\partial^2 U}{\partial Y^2}\right) + Ra\ Pr\ \theta\ \sin\phi, \tag{3.9}$$

$$U\frac{\partial V}{\partial X} + V\frac{\partial V}{\partial Y} = -\frac{\partial P}{\partial Y} + Pr\left(\frac{\partial^2 V}{\partial X^2} + \frac{\partial^2 V}{\partial Y^2}\right) + Ra\ Pr\ \theta\ \cos\phi, \tag{3.10}$$

$$U\frac{\partial \theta}{\partial X} + V\frac{\partial \theta}{\partial Y} = \frac{\partial^2 \theta}{\partial X^2} + \frac{\partial^2 \theta}{\partial Y^2}. \tag{3.11}$$

The dimensionless boundary conditions on each wall of the cavity for velocity and temperature fields are given by

- Temperature is adiabatic along the horizontal walls:

$$U(X,Y) = 0, \quad V(X,Y) = 0, \quad \frac{\partial \theta}{\partial n} = 0 \tag{3.12}$$

- Wall BC is maintained at cold temperature:

$$U(X,Y) = 0, \quad V(X,Y) = 0, \quad \theta = 0 \tag{3.13}$$

- Wall DA is maintained at hot temperature:

$$U(X,Y) = 0, \quad V(X,Y) = 0, \quad \theta = 1 \tag{3.14}$$

  where n denote the normal vector.

3.2 Numerical method of solution

The transformed non-dimensional governing Eqs. (3.8)-(3.11) together with the boundary conditions (3.12)-(3.14) has been carried out numerically by Galerkin finite element method using the bi-quadratic element for velocity and temperature, and discontinuous P_1 element for pressure. First, the weak formulation of the governing equations is derived and then the solution is approximated by using the Galerkin approximation method.

3.2.1 Variational Formulation

The idea of variational formulation is to transform the governing equations into integral equations. The variational formulation of the governing equations is obtained by multiplying with test function and then integrating over the whole domain.

Strong form of governing equations:

$$\frac{\partial U}{\partial X} + \frac{\partial V}{\partial Y} = 0, \tag{3.15}$$

$$U\frac{\partial U}{\partial X} + V\frac{\partial U}{\partial Y} = -\frac{\partial P}{\partial X} + Pr\left(\frac{\partial^2 U}{\partial X^2} + \frac{\partial^2 U}{\partial Y^2}\right) + Ra\ Pr\ \theta\ \sin\phi, \tag{3.16}$$

$$U\frac{\partial V}{\partial X} + V\frac{\partial V}{\partial Y} = -\frac{\partial P}{\partial Y} + Pr\left(\frac{\partial^2 V}{\partial X^2} + \frac{\partial^2 V}{\partial Y^2}\right) + Ra\ Pr\ \theta\ \cos\phi, \tag{3.17}$$

$$U\frac{\partial \theta}{\partial X} + V\frac{\partial \theta}{\partial Y} = \frac{\partial^2 \theta}{\partial X^2} + \frac{\partial^2 \theta}{\partial Y^2}. \tag{3.18}$$

Weak formulation/Variational form:
First, multiply both sides of momentum equations and the temperature equation by the test function $w \in W$ and the continuity equation is multiplied by test function $z \in Q^*$ and then integrate over the whole domain where W and Q^* are test spaces. The test space $W = (H^1(\Omega), H^1(\Omega), H^1(\Omega))$ is considered for the velocity components and temperature, and $Q^* = L^2(\Omega)$ is test space for the pressure term. Thus, the variational/weak formulation of Eqs. (3.15)-(3.18) reads as follows

Find $(U,\ V,\ \theta,\ P) \in W \times Q^*$ such that

$$\int_\Omega \left(U\frac{\partial U}{\partial X} + V\frac{\partial U}{\partial Y}\right) w\ d\Omega - Pr\int_\Omega \left(\frac{\partial^2 U}{\partial X^2} + \frac{\partial^2 U}{\partial Y^2}\right) w\ d\Omega$$
$$- Ra\ Pr\ \sin\ \phi \int_\Omega \theta\ w\ d\Omega + \int_\Omega \frac{\partial P}{\partial X} w\ d\Omega = 0, \tag{3.19}$$

$$\int_\Omega \left(U\frac{\partial V}{\partial X} + V\frac{\partial V}{\partial Y}\right) w\ d\Omega - Pr\int_\Omega \left(\frac{\partial^2 V}{\partial X^2} + \frac{\partial^2 V}{\partial Y^2}\right) w\ d\Omega$$
$$- Ra\ Pr\ \cos\ \phi \int_\Omega \theta\ w\ d\Omega + \int_\Omega \frac{\partial P}{\partial Y} w\ d\Omega = 0, \tag{3.20}$$

$$\int_\Omega \left(\frac{\partial U}{\partial X} + \frac{\partial V}{\partial Y}\right) z\ d\Omega = 0, \tag{3.21}$$

$$\int_\Omega \left(U\frac{\partial \theta}{\partial X} + V\frac{\partial \theta}{\partial Y}\right) w\ d\Omega - \int_\Omega \left(\frac{\partial^2 \theta}{\partial X^2} + \frac{\partial^2 \theta}{\partial Y^2}\right) w\ d\Omega = 0, \tag{3.22}$$

for all $(w,\ z)\ \epsilon\ W \times Q^*$.

In Galerkin discretization, the infinite dimensional test and trial spaces are approximated by the finite dimensional spaces. In particular, following are the trial and test spaces

Trial spaces:

$U \approx U_h, \quad V \approx V_h, \quad \theta \approx \theta_h \quad \text{and} \quad P \approx P_h.$

Test spaces:

$W \approx W_h, \qquad Q^* \approx Q_h^*.$

The Galerkin discretization results into the following non-linear discretized integral equations.

$$Pr \int_\Omega \left(\frac{\partial U_h}{\partial X}\frac{\partial w_h}{\partial X} + \frac{\partial U_h}{\partial Y}\frac{\partial w_h}{\partial Y} \right) d\Omega + \int_\Omega \left(U_h \frac{\partial U_h}{\partial X} + V_h \frac{\partial U_h}{\partial Y} \right) w_h \, d\Omega$$
$$- Ra \; Pr \; \sin\phi \int_\Omega \theta_h \; w_h \; d\Omega + \int_\Omega \frac{\partial P_h}{\partial X} w_h \; d\Omega = 0, \tag{3.23}$$

$$Pr \int_\Omega \left(\frac{\partial V_h}{\partial X}\frac{\partial w_h}{\partial X} + \frac{\partial V_h}{\partial Y}\frac{\partial w_h}{\partial Y} \right) d\Omega + \int_\Omega \left(U_h \frac{\partial V_h}{\partial X} + V_h \frac{\partial V_h}{\partial Y} \right) w_h \, d\Omega$$
$$- Ra \; Pr \; \cos\phi \int_\Omega \theta_h \; w_h \; d\Omega + \int_\Omega \frac{\partial P_h}{\partial Y} w_h \; d\Omega = 0, \tag{3.24}$$

$$\int_\Omega \left(\frac{\partial U_h}{\partial X} + \frac{\partial V_h}{\partial Y} \right) z_h \; d\Omega = 0, \tag{3.25}$$

$$\int_\Omega \left(\frac{\partial \theta_h}{\partial X}\frac{\partial w_h}{\partial X} + \frac{\partial \theta_h}{\partial Y}\frac{\partial w_h}{\partial Y} \right) d\Omega + \int_\Omega \left(U_h \frac{\partial \theta_h}{\partial X} + V_h \frac{\partial \theta_h}{\partial Y} \right) w_h \, d\Omega = 0, \tag{3.26}$$

In the next step, discretized test and trial functions are approximated by using the finite element approximations. Solving the above system of discrete integral equations lead to the following block matrix.

$$\underbrace{\begin{bmatrix} Pr\; L^* + N(\underline{U},\underline{V}) & O & B_1 & -Ra\; Pr\; \sin\phi\; M \\ O & Pr\; L^* + N(\underline{U},\underline{V}) & B_2 & -Ra\; Pr\; \cos\phi\; M \\ B_1^T & B_2^T & O & O \\ O & O & O & L^* + N(\underline{U},\underline{V}) \end{bmatrix}}_{\mathbf{A}} \underbrace{\begin{bmatrix} \underline{U} \\ \underline{V} \\ \underline{P} \\ \underline{\theta} \end{bmatrix}}_{\mathbf{U}} = \underbrace{\begin{bmatrix} \underline{0} \\ \underline{0} \\ \underline{0} \\ \underline{0} \end{bmatrix}}_{\mathbf{F}} \tag{3.27}$$

In the block matrix (3.27), L^* is the Laplace marix, M is mass matrix, N is the convective matrix and O is the zero matrix. B_1 and B_2 are the pressure matrices and B_1^T, B_2^T are their corresponding transpose matrices. Velocity components and temperature are discretized by Q_2-element of 3rd order accuracy and pressure is approximated by P_1^{disc}-element of 1st order accuracy (see [42] for details). The coupled non-linear equations are linearized by the Picard iteration method and Guassian elimination method is utilized

to solve the associated linear subproblems. Some tolerance value for the convergence of iterative scheme is prescribed to see the absolute difference of the two consecutive iteration values to the preceding iteration values. The stopping criterion to the iterative scheme is given by

$$\left| \frac{\Psi^{n+1} - \Psi^{n}}{\Psi^{n+1}} \right| \leq 10^{-6}. \tag{3.28}$$

Here Ψ is used to represent U, V, P, θ, where the superscript n denotes the iteration number.

3.3 Code Validation

In order to validate the code adopted for the numerical solution of equations governing the natural convective flow, the comparison of current results with some of the earlier published work on free convection [43–46] are displayed in Table 3.1. Results obtained from the current code are in good agreement with the published results [43–46].

TABLE 3.1: Comparison of current code results with some earlier results of [43–46].

Raleigh number	Present study	Ref [43]	Ref [44]	Ref [45]	Ref [46]
10^3	1.118	1.117	1.121	1.118	1.115
10^4	2.245	2.246	2.286	2.243	2.226
10^5	4.522	4.518	4.546	4.519	4.508

3.4 Results and discussion

Galerkin weighted residual method is utilized to solve the equations governing the heat transfer and fluid flow. The obtained numerical results are visualized by means of streamlines and isotherms in the square inclined cavity which can be seen through Figures 3.2-3.4. The cavity for the given problem is considered with two adiabatic walls AB and CD, whereas the wall DA is kept at maximum temperature and the wall BC is kept cold. Effect of the governing parameters such as Prandtl number, Raleigh number

and inclination angle on the for various considered values is observed.

Figure 3.2(a)-(d) illustrates the effect of the variation of the inclination angles ($\phi = 15°$, 30° 60° and 75°) on fluid flow in an inclined cavity with $Ra = 10^3$ and $Pr = 0.025$. At $Ra = 10^3$, the isotherms are found to be slightly curved nature due to inclination angle effect. For all inclination angles, the isotherms are flattened near the top section of wall BC (cold wall) and lower section of wall DA (hot wall). Flow of the fluid inside the square cavity is weak which can be viewed by the low intensity of streamlines. The flow strength with augmentation in inclination angle decreases at low Raleigh number as $|\psi|_{max} = 1.21$, 1.20, 0.88 and 0.51 for $\phi = 15°$, 30°, 60° and 75°, respectively. The flow strength increases with an increment in the Raleigh number due to onset of convection. At $Ra = 10^4$ and $Pr = 0.025$, the isotherms in core of the cavity are gradually contorted for all inclination angles. The convection starts gradually inside the cavity for $Ra = 10^4$.

Figure 3.3(a)-(d) depicts the fluid flow for $Ra = 10^5$ and $Pr = 0.025$ inside the cavity by varying the inclination angles. The buoyancy driven forces with the Raleigh number increase and thus convection at high Ra ($Ra = 10^5$) dominates in the cavity. At $Ra = 10^5$, it is observed that the isotherms are extremely distorted for all inclination angles at the centre portion of the cavity due to the dominance of convection. In contrast to the previous case ($Ra = 10^3$), the isotherms for all ϕ are found to be compressed at the top of wall BC (cold wall) and at the bottom of left wall DA (hot wall). The streamline contours follow the similar circular pattern as in the previous case ($Ra = 10^3$). The flow intensity inside the cavity increases, irrespective of ϕ which can be visualized by the maximum magnitude of the streamlines. The values of $|\psi|_{max}$ at $Ra = 10^5$ are 10.4, 14.4, 21.9 and 23.5 for $\phi = 15°$, 30°, 60° and 75°, respectively (see Figure 3.3(a)-(c)).

Figure 3.4(a)-(d) shows the effect of various inclination angles on isotherms and streamlines at $Ra = 10^5$ and $Pr = 998$. It is observed that the isotherms at the lower section of the wall DA and at the upper section of the cold wall BC are highly compressed for all values of the inclination angle ϕ. It may be seen that the streamline contours appear in the shape of cavity near the walls, which contrasts the previous case with $Ra = 10^3$ where it was observed in circular pattern. The streamlines at the center of the cavity occur in almost elliptical shape for $\phi = 30°$ 60° and 75°, whereas dumbbell shape is observed in streamlines at $\phi = 15°$. The maximum magnitude of streamlines indicates

that the fluid flow intensity inside the cavity is high as compared with the previous case ($Pr = 0.025$) for all values of ϕ. At high Prandtl number ($Pr = 998$), the values observed for $|\psi|_{max}$ are 14.1, 17.3, 23.3 and 24.6 for $\phi = 15°$, $30°$, $60°$ and $75°$, respectively.

The influence of the physical parameters i.e., Raleigh number ($Ra = 10^3$) and Prandtl number ($Pr = 0.025$ and 998) with the varying inclination angle ϕ on the heat transfer is illustrated in Figure 4.5. For low Raleigh number ($Ra = 10^3$), the declination in the graph of average Nusselt number has been observed for all inclination angles.

In Figure 4.6, the average heat transfer against the inclination angle φ and physical parameters i.e., Raleigh number ($Ra = 10^5$) and Prandtl number ($Pr = 0.025$ and 998) is plotted. At $Pr = 0.025$, the enhancement in average Nusselt number has been observed for $\phi = 15°$ - $60°$ and it decreases for $\phi = 75°$. For the case of high Prandtl number, the rate of heat transfer enhanced for small inclination angles whereas the opposite effect has been observed for the large values of ϕ.

The effect of the varying Raleigh number on the heat transfer rates is depicted in Figure 4.7. An augmentation in the average Nusselt number is observed for both cases of Prandtl number. Maximum values of heat transfer rate are found at high Raleigh number (i.e. $Ra = 10^5$) due to strong convection.

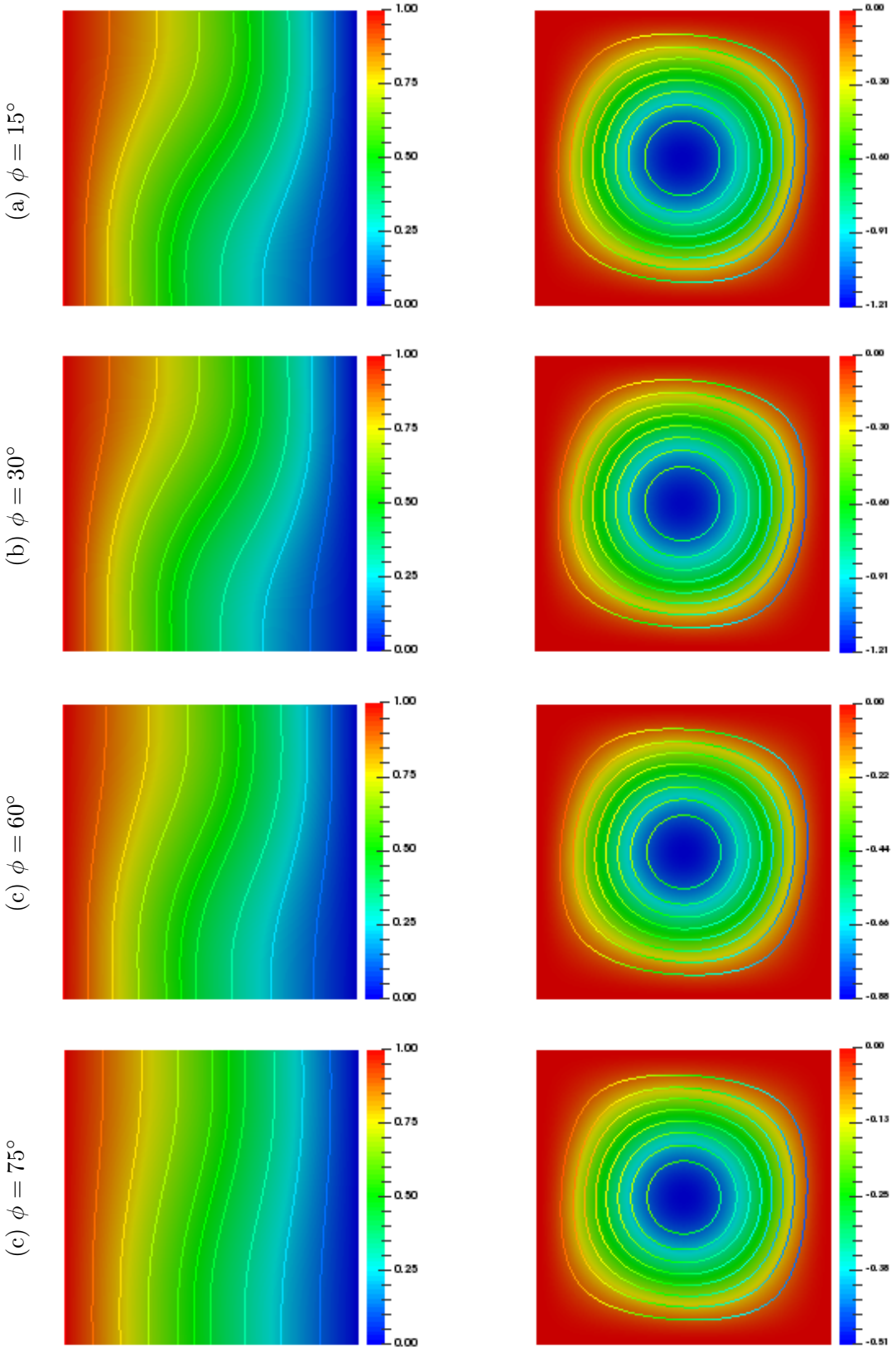

FIGURE 3.2: Influence of inclination angle on isotherms (left) and streamlines (right) for $Ra = 10^3$ and $Pr = 0.025$.

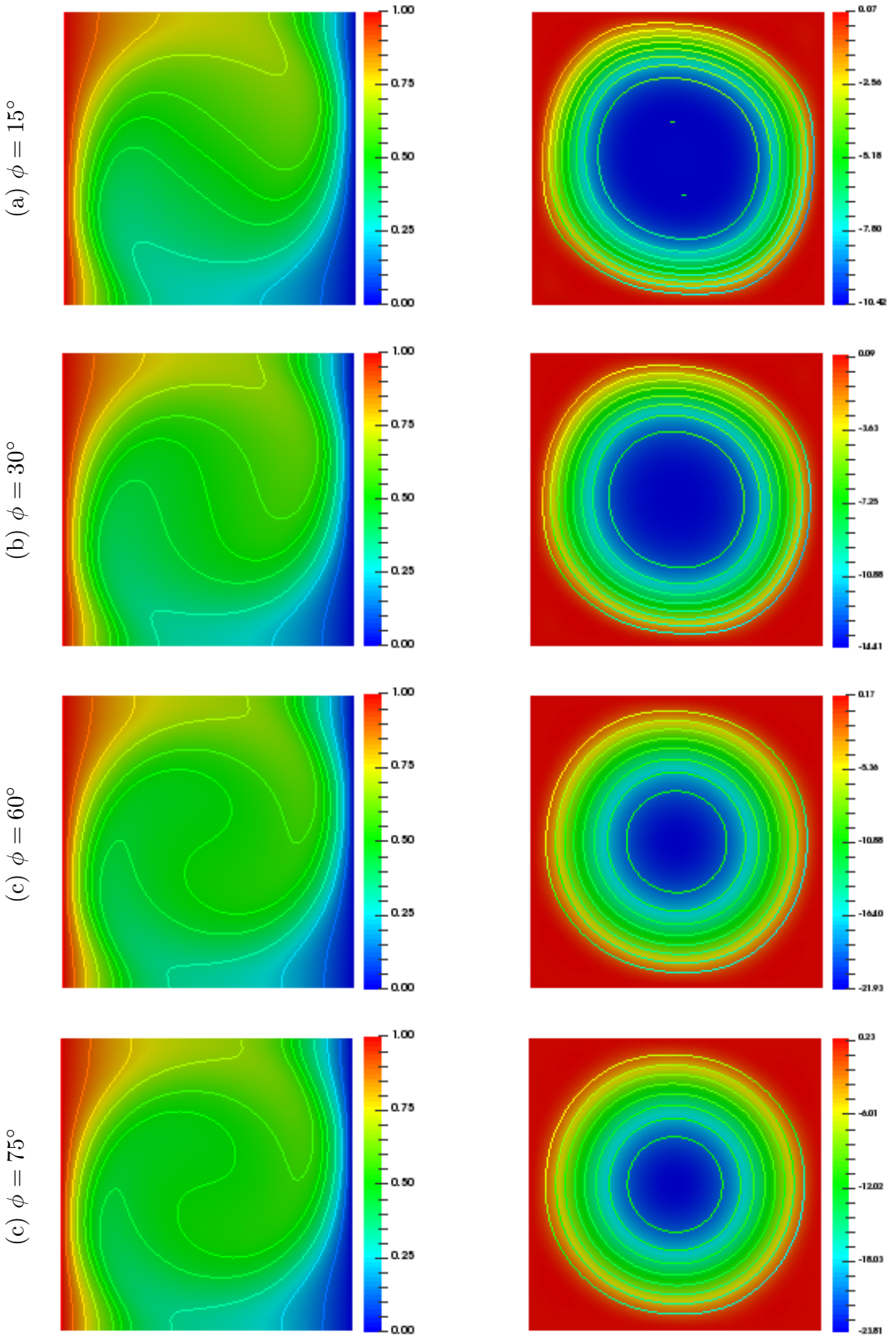

FIGURE 3.3: Influence of inclination angle on isotherms (left) and streamlines (right) for $Ra = 10^5$ and $Pr = 0.025$.

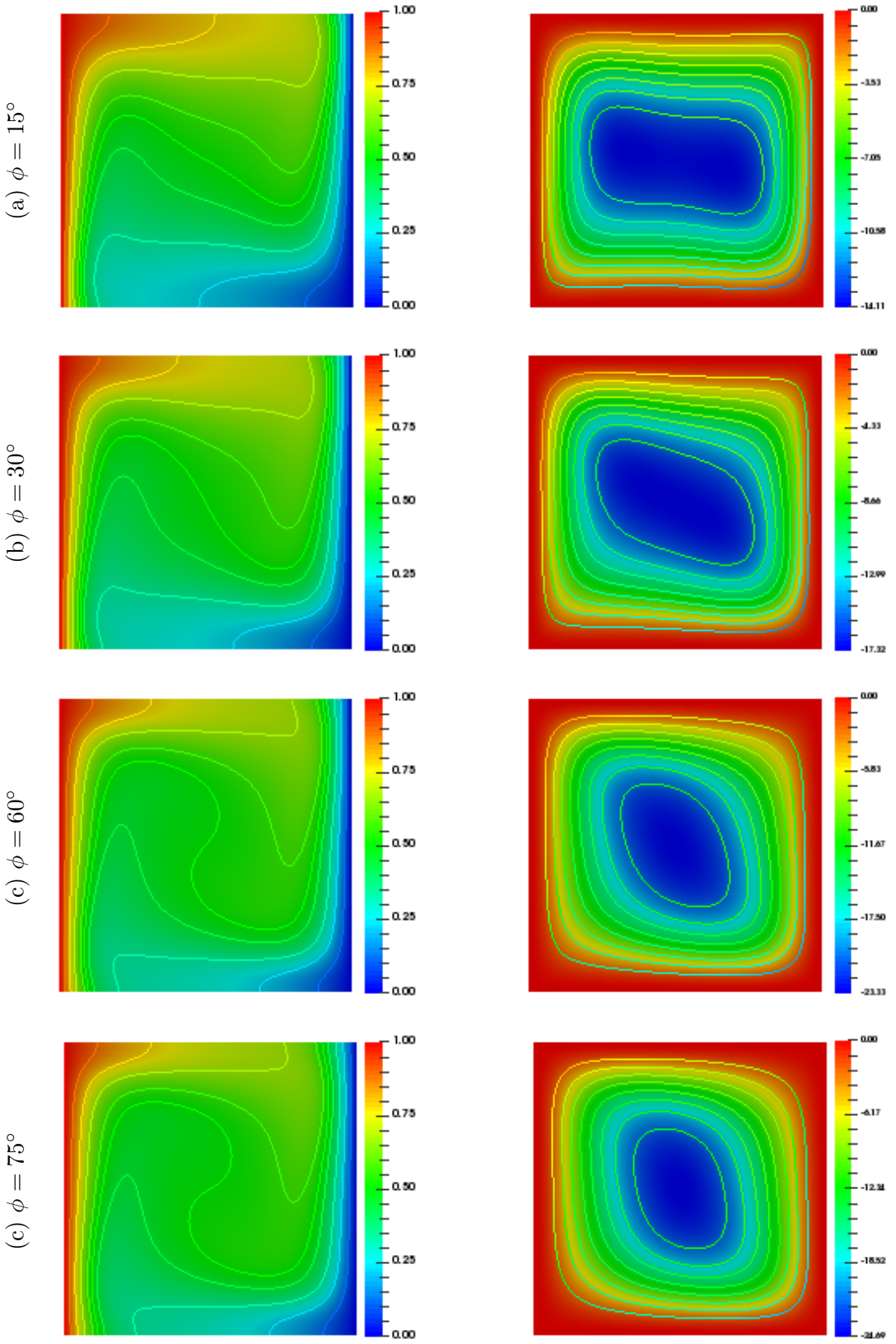

FIGURE 3.4: Influence of inclination angle on isotherms (left) and streamlines (right) for $Ra = 10^5$ and $Pr = 998$.

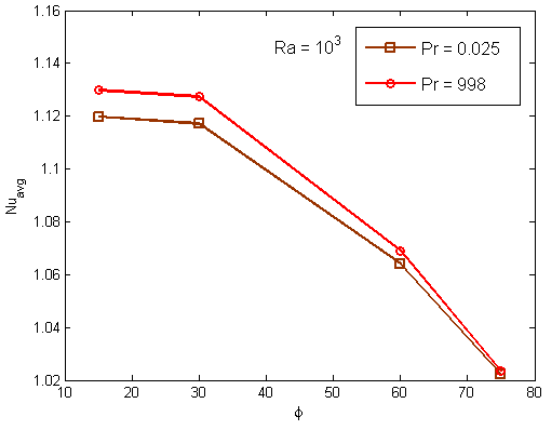

FIGURE 3.5: The influence of inclination angle with $Ra = 10^3$ and Pr on Nusselt number.

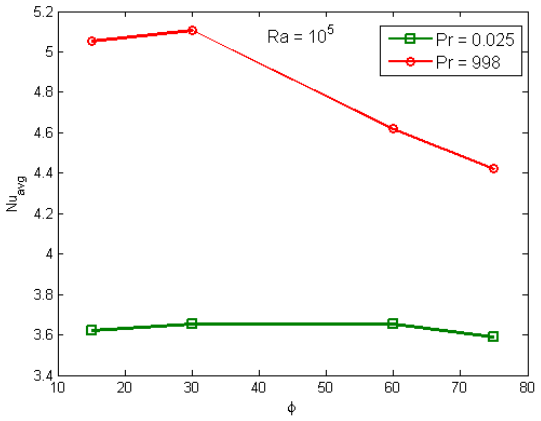

FIGURE 3.6: The influence of inclination angle with $Ra = 10^5$ and Pr on Nusselt number.

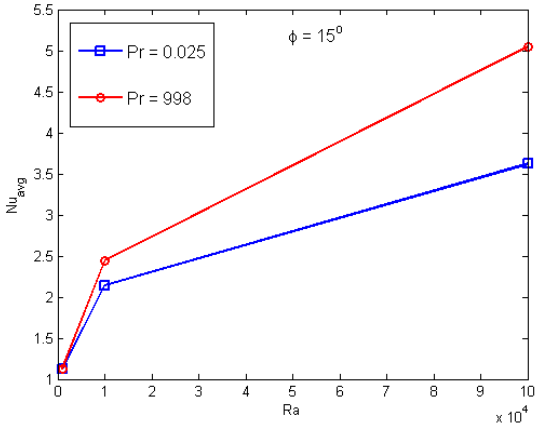

FIGURE 3.7: The influence of Raleigh number with $\phi = 15^o$ and Pr on Nusselt number.

Chapter 4

Simulations of natural convective flow considering internal heat generation/absorption

Many researchers have analyzed the study of natural convective flow. Previously, effects of different physical parameters and inclination angles have been observed but despite of all the great work has been done, there is certainly a less information regarding natural convective flow with internal heat generation/absorption inside the inclined square enclosure. In this chapter, the inspirational work of Basak *et al.* [38] is extended. The main purpose of the current project is to asses and analyze the impact of internal heat genration/absorption on heat transfer by means of isotherms and fluid flow via streamlines.

In this chapter, we investigate the influence of heat generation/absorption on the steady and incompressible natural convective flow in a square tilted cavity. In order to solve the governing equations, the dimensionless form of the system of equations is obtained by using a suitable transformation. This system of dimensionless coupled partial differential equations is approximated by utilizing a well known Galerkin finite element technique. Impact of internal heat generation/absorption parameter on flow and heat exchange is viewed by some useful plots and analyzed by isotherms and streamlines. This chapter is an extension of the work presented in Chapter 3.

4.1 Mathematical Formulation

The two dimensional, steady and incompressible natural convective flow with internal heat generation/absorpion in tilted square cavity is considered. Two horizontal walls (AB and CD) of the cavity are assumed to be adiabatic with the left hot and the right cold wall. The enclosure is skewed at an angle ϕ° with horizontal coordinate. Under these assumptions, the equations of continuity, momentum and energy equation with internal heat generation takes the following form.

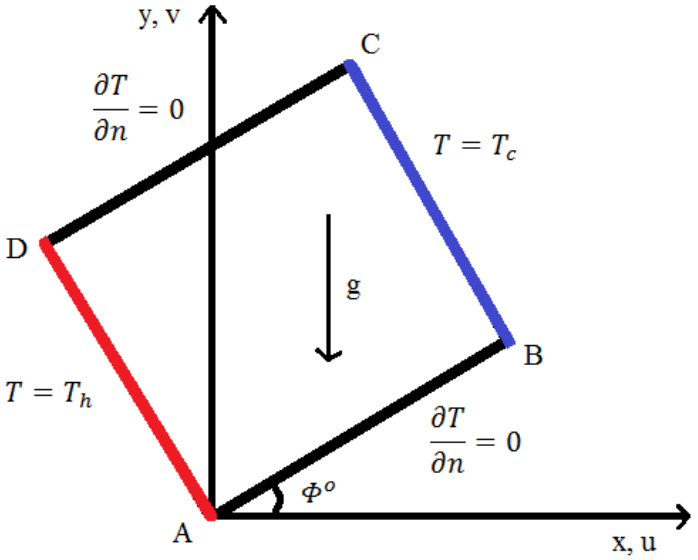

FIGURE 4.1: Geometry of the problem.

Continuity equation:

$$\frac{\partial u}{\partial x} + \frac{\partial v}{\partial y} = 0, \tag{4.1}$$

x-momentum equation:

$$u\frac{\partial u}{\partial x} + v\frac{\partial u}{\partial y} = -\frac{1}{\rho}\frac{\partial p}{\partial x} + \nu\left(\frac{\partial^2 u}{\partial x^2} + \frac{\partial^2 u}{\partial y^2}\right) + g\beta(T - T_c)\sin\phi, \tag{4.2}$$

y-momentum equation:

$$u\frac{\partial v}{\partial x} + v\frac{\partial v}{\partial y} = -\frac{1}{\rho}\frac{\partial p}{\partial y} + \nu\left(\frac{\partial^2 v}{\partial x^2} + \frac{\partial^2 v}{\partial y^2}\right) + g\beta(T - T_c)\cos\phi, \tag{4.3}$$

Energy equation:

$$u\frac{\partial T}{\partial x}+v\frac{\partial T}{\partial y}=\alpha\left(\frac{\partial^2 T}{\partial x^2}+\frac{\partial^2 T}{\partial y^2}\right)+\frac{Q_0}{\rho c_p}(T-T_c). \tag{4.4}$$

In the above system of equations, ν represents the kinematic fluid viscosity, ρ is fluid density, c_p is the specific heat, Q_0 is the heat flux, α is the thermal diffusivity, the expansion coefficient is β, ϕ is an inclination angle, fluid temperature is T and T_c is the cold right wall temperature, acceleration due to gravity is g, p is pressure of the fluid and u,v denote the components of velocity.

Following are the boundary conditions for the dimensional velocity and temperature.

- On the horizontal walls AB and CD:

$$u(x,y)=0,\quad v(x,y)=0,\quad \frac{\partial T}{\partial n}=0 \tag{4.5}$$

- On the right wall BC:

$$u(x,y)=0,\quad v(x,y)=0,\quad T=T_c \tag{4.6}$$

- On the left Wall DA:

$$u(x,y)=0,\quad v(x,y)=0,\quad T=T_h \tag{4.7}$$

where n denote the normal vector.

4.1.1 Dimensionless form of the Governing Equations

By using the following dimensionless parameters [38], Eqs. (4.1)-(4.4) are converted into the dimensionless form as follows.

$$X=\frac{x}{L},\qquad Y=\frac{y}{L},\qquad U=\frac{uL}{\alpha},\qquad V=\frac{vL}{\alpha},\qquad P=\frac{pL^2}{\rho\alpha^2},\qquad \theta=\frac{T-T_c}{T_h-T_c}$$

$$Pr=\frac{\nu}{\alpha},\qquad Ra=\frac{g\beta(T_h-T_c)L^3Pr}{\nu^2},\qquad q^*=\frac{Q_0L^2}{\rho c_p\alpha}.$$

The transformed dimensionless governing reads the following.

$$\frac{\partial U}{\partial X} + \frac{\partial V}{\partial Y} = 0, \tag{4.8}$$

$$U\frac{\partial U}{\partial X} + V\frac{\partial U}{\partial Y} = -\frac{\partial P}{\partial X} + Pr\left(\frac{\partial^2 U}{\partial X^2} + \frac{\partial^2 U}{\partial Y^2}\right) + Ra\ Pr\ \theta\ \sin\phi, \tag{4.9}$$

$$U\frac{\partial V}{\partial X} + V\frac{\partial V}{\partial Y} = -\frac{\partial P}{\partial Y} + Pr\left(\frac{\partial^2 V}{\partial X^2} + \frac{\partial^2 V}{\partial Y^2}\right) + Ra\ Pr\ \theta\ \cos\phi, \tag{4.10}$$

$$U\frac{\partial \theta}{\partial X} + V\frac{\partial \theta}{\partial Y} = \frac{\partial^2 \theta}{\partial X^2} + \frac{\partial^2 \theta}{\partial Y^2} + q^*\ \theta. \tag{4.11}$$

Following are the dimensionless boundary conditions for velocity and temperature fields along each side of the cavity.

- Temperature is adiabatic along the horizontal walls:

$$U(X,Y) = 0, \quad V(X,Y) = 0, \quad \frac{\partial \theta}{\partial n} = 0 \tag{4.12}$$

- Wall BC is maintained cold:

$$U(X,Y) = 0, \quad V(X,Y) = 0, \quad \theta = 0 \tag{4.13}$$

- Wall DA is maintained hot:

$$U(X,Y) = 0, \quad V(X,Y) = 0, \quad \theta = 1 \tag{4.14}$$

  where n is the normal vector.

4.2 Numerical Solution

The system of dimensionless governing Eqs. (4.8)-(4.11) together with the boundary conditions (4.12)-(4.14) has been solved numerically by finite element method with Galerkin weighted residual method.

4.2.1 Variational Formulation

Finding a solution in strong form is not always possible and there may not be a smooth solution to a particular problem. In order to overcome these difficulties, weak formulation is preferred. Weak formulation minimize the continuity or smoothness requirements on approximation functions. The main concept of weak/variational formulation is to turn the governing equations into integral equations. For the derivation of weak form, the governing equations are first multiplied by the test function obtained and then integration is performed over the entire domain.

Let $W = (H^1(\Omega))^3$ and $Q^* = L^2(\Omega)$ be the test spaces for velocity components, temperature and pressure respectively. The variational formulation of the governing Eqs. (4.8)-(4.11) reads the following

Find $(U,\, V,\, \theta,\, P) \in W \times Q^*$ such that

$$\int_\Omega \left(U\frac{\partial U}{\partial X} + V\frac{\partial U}{\partial Y}\right) w \; d\Omega - Pr \int_\Omega \left(\frac{\partial^2 U}{\partial X^2} + \frac{\partial^2 U}{\partial Y^2}\right) w \; d\Omega$$
$$- Ra \; Pr \; \sin\phi \int_\Omega \theta \; w \; d\Omega + \int_\Omega \frac{\partial P}{\partial X} w \; d\Omega = 0, \tag{4.15}$$
$$\int_\Omega \left(U\frac{\partial V}{\partial X} + V\frac{\partial V}{\partial Y}\right) w \; d\Omega - Pr \int_\Omega \left(\frac{\partial^2 V}{\partial X^2} + \frac{\partial^2 V}{\partial Y^2}\right) w \; d\Omega$$
$$- Ra \; Pr \; \cos\phi \int_\Omega \theta \; w \; d\Omega + \int_\Omega \frac{\partial P}{\partial Y} w \; d\Omega = 0, \tag{4.16}$$
$$\int_\Omega \left(\frac{\partial U}{\partial X} + \frac{\partial V}{\partial Y}\right) z \; d\Omega = 0, \tag{4.17}$$
$$\int_\Omega \left(U\frac{\partial \theta}{\partial X} + V\frac{\partial \theta}{\partial Y}\right) w \; d\Omega - \int_\Omega \left(\frac{\partial^2 \theta}{\partial X^2} + \frac{\partial^2 \theta}{\partial Y^2}\right) w \; d\Omega - q^* \int_\Omega \theta \; w \; d\Omega = 0. \tag{4.18}$$

for all $(w,\, z) \; \epsilon \; W \times Q^*$.

The infinite dimensional test and trial spaces are approximated to finite dimensional spaces using Galerkin method. Following are the approximations

$U \approx U_h, \quad V \approx V_h, \quad \theta \approx \theta_h \quad$ and $\quad P \approx P_h$

$W \approx W_h, \qquad Q^* \approx Q_h^*$

Using the Galerkin approximation in Eqs. (4.15)-(4.18), we get

$$Pr \int_\Omega \left(\frac{\partial U_h}{\partial X}\frac{\partial w_h}{\partial X} + \frac{\partial U_h}{\partial Y}\frac{\partial w_h}{\partial Y} \right) d\Omega + \int_\Omega \left(U_h \frac{\partial U_h}{\partial X} + V_h \frac{\partial U_h}{\partial Y} \right) w_h \, d\Omega$$
$$- Ra \; Pr \; \sin\phi \int_\Omega \theta_h \; w_h \; d\Omega + \int_\Omega \frac{\partial P_h}{\partial X} w_h \; d\Omega = 0, \tag{4.19}$$

$$Pr \int_\Omega \left(\frac{\partial V_h}{\partial X}\frac{\partial w_h}{\partial X} + \frac{\partial V_h}{\partial Y}\frac{\partial w_h}{\partial Y} \right) d\Omega + \int_\Omega \left(U_h \frac{\partial V_h}{\partial X} + V_h \frac{\partial V_h}{\partial Y} \right) w_h \, d\Omega$$
$$- Ra \; Pr \; \cos\phi \int_\Omega \theta_h \; w_h \; d\Omega + \int_\Omega \frac{\partial P_h}{\partial Y} w_h \; d\Omega = 0, \tag{4.20}$$

$$\int_\Omega \left(\frac{\partial U_h}{\partial X} + \frac{\partial V_h}{\partial Y} \right) z_h \; d\Omega = 0, \tag{4.21}$$

$$\int_\Omega \left(\frac{\partial \theta_h}{\partial X}\frac{\partial w_h}{\partial X} + \frac{\partial \theta_h}{\partial Y}\frac{\partial w_h}{\partial Y} \right) d\Omega + \int_\Omega \left(U_h \frac{\partial \theta_h}{\partial X} + V_h \frac{\partial \theta_h}{\partial Y} \right) w_h \, d\Omega - q^* \int_\Omega \theta_h \; w_h \; d\Omega = 0. \tag{4.22}$$

Substituting the approximate(or basis) functions for U_h, V_h, P_h and θ_h, the above system of equations yield the following block matrix.

$$\underbrace{\begin{bmatrix} Pr\; L^* + N(\underline{U},\underline{V}) & O & B_1 & -Ra\; Pr\; \sin\phi\; M \\ O & Pr\; L^* + N(\underline{U},\underline{V}) & B_2 & -Ra\; Pr\; \cos\phi\; M \\ B_1^T & B_2^T & O & O \\ O & O & O & L^* + q^*\; M + N(\underline{U},\underline{V}) \end{bmatrix}}_{\mathbf{A}} \underbrace{\begin{bmatrix} \underline{U} \\ \underline{V} \\ \underline{P} \\ \underline{\theta} \end{bmatrix}}_{\mathbf{U}} = \underbrace{\begin{bmatrix} \underline{0} \\ \underline{0} \\ \underline{0} \\ \underline{0} \end{bmatrix}}_{\mathbf{F}} \tag{4.23}$$

Laplace matrix, mass matrix, convective matrix and zero matrix in the block matrix (4.23) are denoted by L^*, M, N and O, respectively. B_1 and B_2 are the pressure matrices where the matrices B_1^T and B_2^T are their corresponding transpose matrices. Q_2 (or biquadratic) element is used to discretize the temperature and velocity components where pressure term is approximated by P_1^{disc} element (see [42] for details). The non-linear system of governing equations are linearized by means of the Picard iteration method and the associated linear subproblems are solved using Guassian elimination method. The stopping criterion to the iterative scheme for the convergence of solution is given by

$$\left| \frac{\Psi^{n+1} - \Psi^n}{\Psi^{n+1}} \right| \leq 10^{-6}. \tag{4.24}$$

In the above defined expression, Ψ denotes U, V, P, θ and the superscript n is used for the iteration number.

4.3 Results and Discussion

The governing equations for the given flow are solved utilizing the Galerkin finite element method. Simulations are performed and the results are exhibited in square enclosure with inclination effect by means of isotherms and streamlines. The cavity under consideration has two vertical walls with thermal boundary conditions and the two horizontal walls under the adiabatic condition. Impact of the various parameters is observed on the flow with the specified values such as Prandtl number ($Pr = 0.025$), Raleigh number ($Ra = 10^2 - 10^5$) and internal heat generation/absorption (q^*= -10, -5, 0 and 5) with inclination angle ($\phi = 15°$, $30°$, $60°$ and $75°$).

Figure 4.1(a)-(d) depicts the effect of Raleigh numbers ($Ra = 10^2 - 10^5$) on flow in square tilted cavity while other parameters are kept fixed such as Prandtl number ($Pr = 0.025$) and heat generation parameter ($q^* = -5$) with inclination angle ($\phi = 15°$). From Figure 4.1(a), it can be seen that the hot fluid rises to the wall DA of the cavity due to the inclination effect of the enclosure. In this case, the transfer of heat is mainly due to conduction as the isotherm contours are uniformly distributed. Due to conduction dominant heat transfer, it is observed that the magnitude of streamines is very low. Enhancement in the Raleigh number causes a curvature in the isotherms which can be seen through Figure 4.1(b). It may also be noted that the isotherms are semi-parallel to walls DA and BC of the cavity. A slight increment in the intensity of streamlines is also noticed. The convection heat transfer mode begins at $Ra = 10^4$ due to which disturbance in the streamlines occur at the middle portion of the cavity. Further, enhanced convection patterns occur inside the cavity for high Ra (i.e. $Ra = 10^5$) and high deformation in the isotherm contours occur at the core of cavity due to dominance of convection. In all cases, streamlines occur almost in a circular shape inside the cavity. The strength of fluid flow enhanced inside the cavity with increase in Ra which is evident from the maximum magnitude of streamfuntion (see Figure 4.1(a)-(d)). For all considered cases the values noticed for $|\psi|_{max}$ are 0.11, 1.09, 5.73 and 11.33 for $Ra = 10^2$, 10^3, 10^4 and 10^5, respectively.

Impact of the varying inclination angles on isotherms and streamlines in square inclined enclosure with $Pr = 0.025$, $Ra = 10^5$ and $q^* = -5$ is illustrated in Figure 4.2(a)-(c). With the enhancement in inclination angle ϕ, the streamfunction grows in magnitude which shows that the flow strength inside the cavity increases as $|\psi|_{max} = 11.3$, 15.41, 22.1 and 23.7 for $\phi = 15°$, $30°$, $60°$ and $75°$, respectively (see Figure 4.2(a)-(d)). For all ϕ, it is observed that isotherms near the top portion of right wall BC and at the bottom portion of wall DA are highly compressed. The contours of isotherm follow almost the similar pattern for all values of inclination angle.

Effect of internal heat generation ($q^* > 0$) or absorption parameter ($q^* < 0$) on streamlines and isotherms distribution with $Pr = 0.025$, $Ra = 10^5$ and $\phi = 15°$ is displayed in Figure 4.3(a)-(c). It is noticed that the fluid temperature in the presence of heat generation parameter increases in the boundary layer of the heated wall whereas the opposite effect has been observed for the heat absorption; namely, thickness of the thermal boundary layer decreases with the decrease in heat absorption parameter. In fact, heat generation process produces hot layer of the fluid near surface resulting increase in the fluid temperature and decrease in the rate of heat transfer. Overall, the heat transfer rates deteriorates with an increase in q^* and it increases with an increases in the heat absorption parameter (negative values). The heat generation/absorption parameter (q^*) has a slight effect on streamline contours (see Figure 4.3(a)-(d)).

The impact of Raleigh number for different cases of heat generation/absorption parameter on the heat transfer rate can be visualized through Figure 4.5. Values of Prandtl number and inclination angle are kept fixed i.e., $Pr = 0.025$ and $\phi = 15°$. The increment in average Nusselt number is observed by increasing the Raleigh number. This is due to the fact that convection is dominant inside the cavity for high Raleigh numbers ($Ra \geq 10^4$) resulting increase in the rate of heat transfer.

In Figure 4.6, the variation in inclination angle against average Nusselt number has been depicted. The average Nusselt number first increases for inclination angles $\phi = 15°$, $30°$ then a slight decrease is observed for $\phi = 60°$ and it further decreases for $\phi = 75°$.

The effect of heat generation/absorption parameter on average Nusselt number for various cases of Ra is shown in Figure 4.7. For all cases it is seen that the average Nusselt number increases for $q^* < 0$ while reduction is observed for $q^* > 0$. In other words, the heat flow decreasing continuously by increasing the value of q^* from $q^* = -10$ to 5.

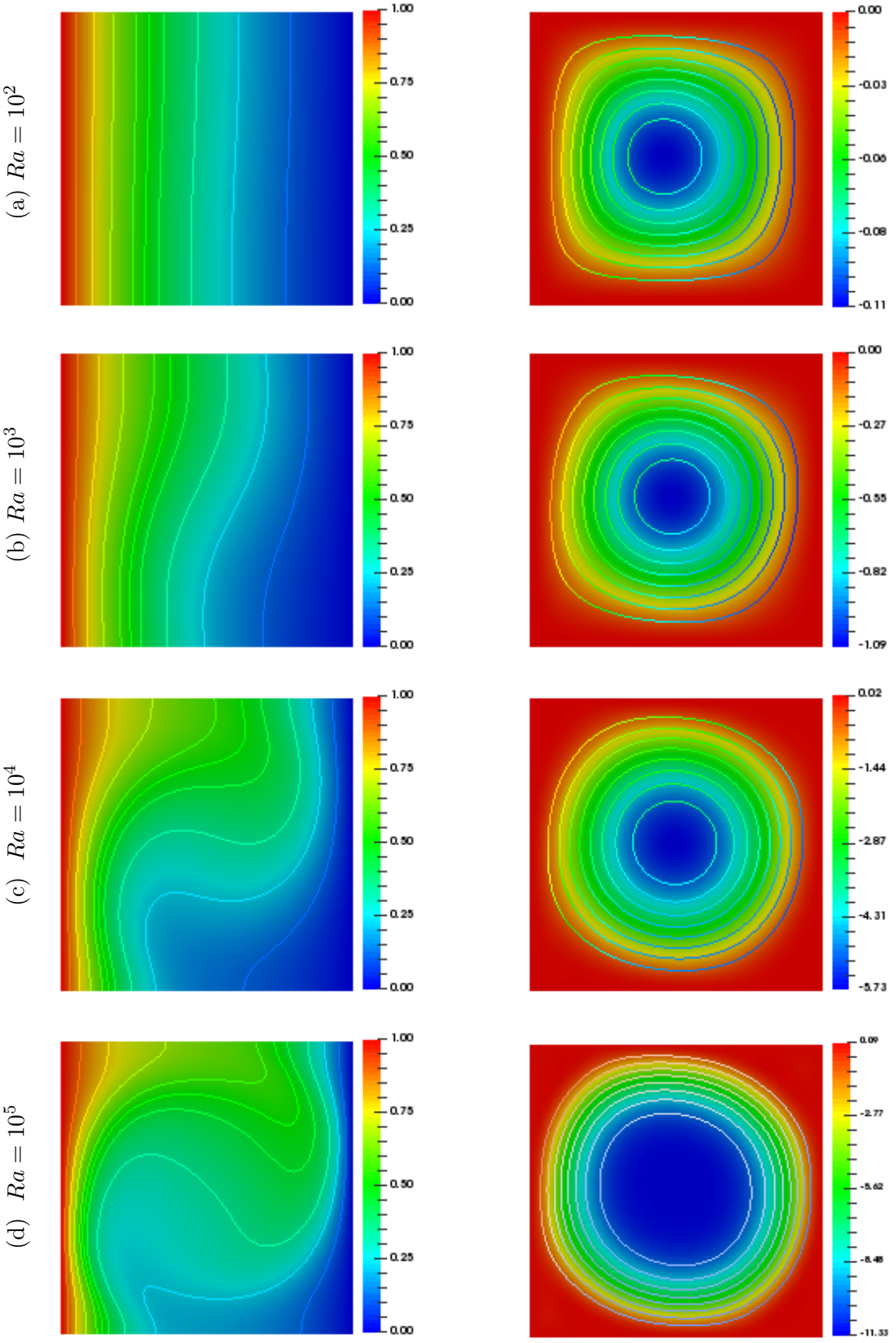

FIGURE 4.2: Influence of Raleigh number on isotherms (left) and streamlines (right) for $Pr = 0.025$, $\phi = 15°$ and $q^* = -5$.

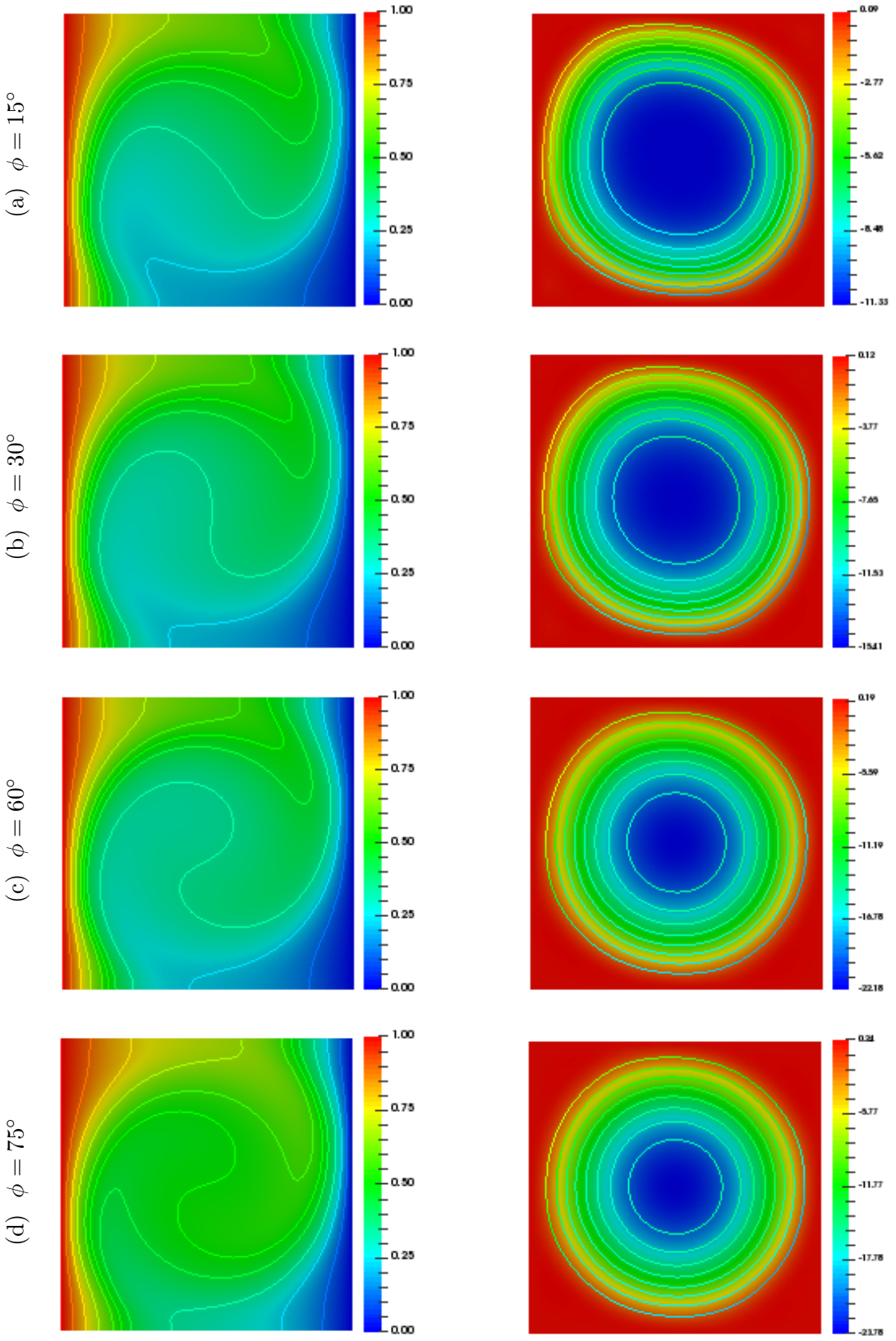

FIGURE 4.3: Influence of inclination angle on isotherms (left) and streamlines (right) for $Pr = 0.025$, $Ra = 10^5$ and $q^* = -5$.

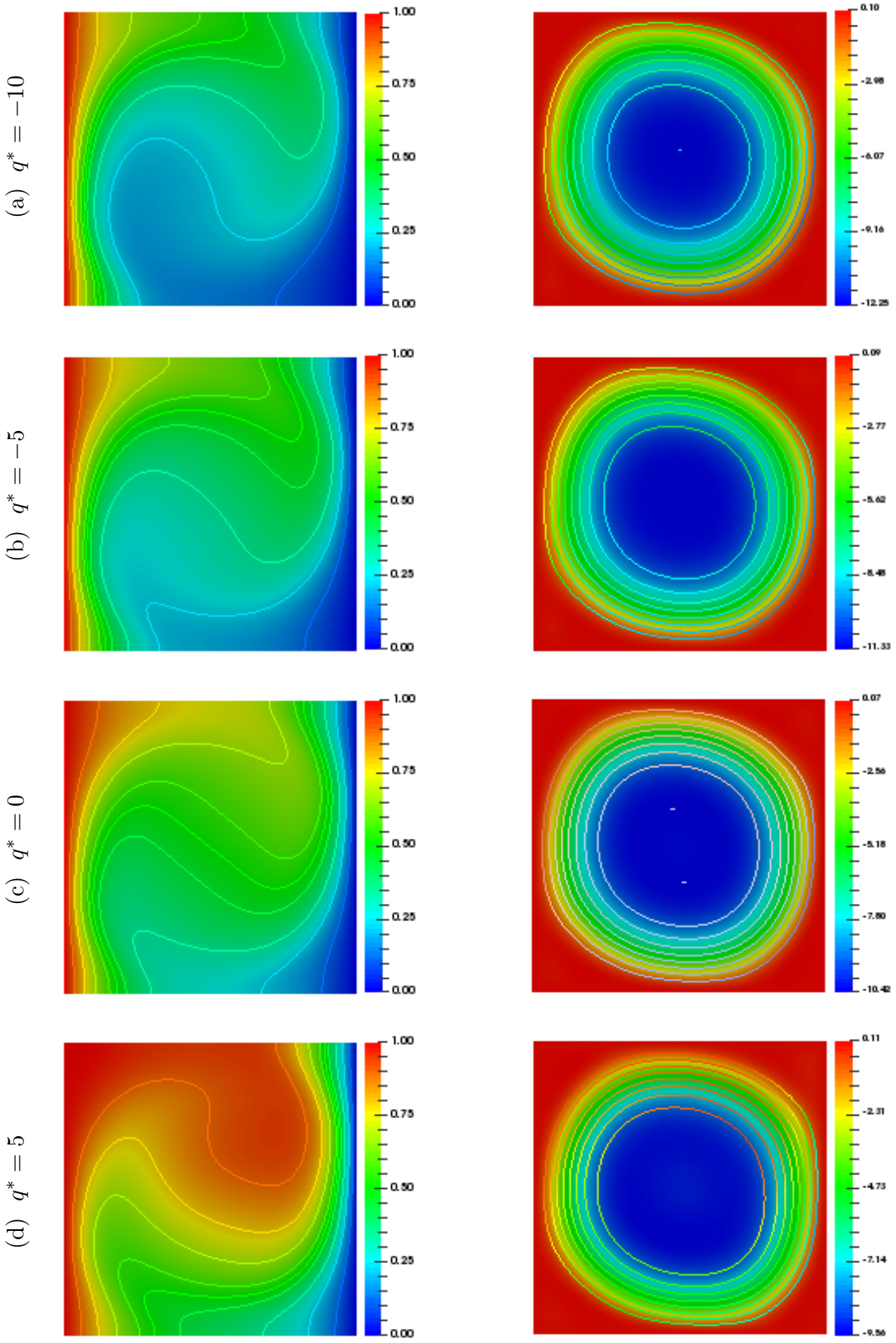

FIGURE 4.4: Influence of heat gneration/absorption parameter on isotherms (left) and streamlines (right) for $Pr = 0.025$, $Ra = 10^5$ and $\phi = 15°$.

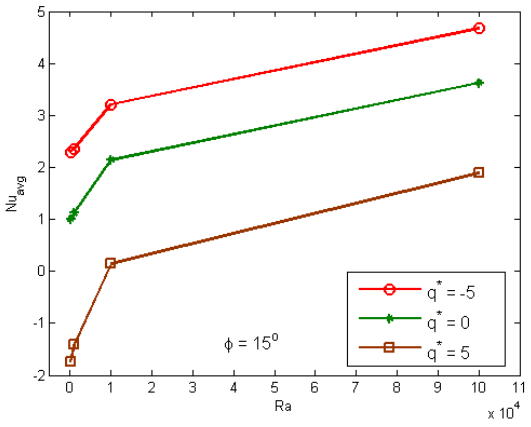

FIGURE 4.5: The influence of Raleigh number on average Nusselt number.

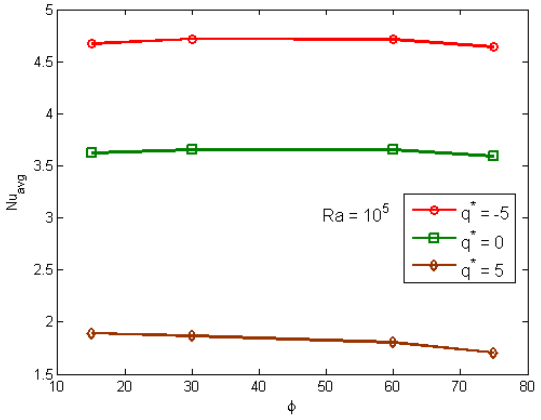

FIGURE 4.6: The influence of inclination angle on average Nusselt number.

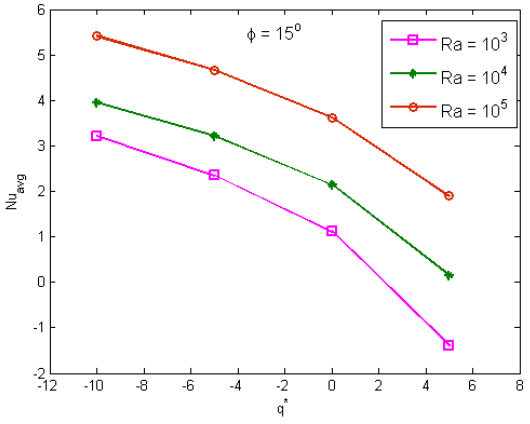

FIGURE 4.7: The influence of heat generation/absorption on average Nusselt number.

Chapter 5

Conclusion

In this dissertation, the study of two dimensional steady and incompressible natural convection flow under the influence of internal heat generation/absorption parameter is carried out in a tilted square cavity. The cavity is considered with two adiabatic walls at the top and bottom, hot wall at the left and cold wall at the right side (see Figure 4.1). The major equations developed for the heat exchange and fluid flow are first transformed into dimensionless form by using an appropriate transformation and then solved numerically by employing the Galerkin finite element method. The finite element Q_2 (biquadratic element) is used for velocity and temperature and P_1^{disc} is for pressure term. The effect of emerging parameters such as Raleigh number, Prandtl number and heat generation/absorption with the inclination angle on the heat transfer and fluid flow has been thoroughly observed. The numerical simulations of the dimensionless velocity and temperature are analyzed by the streamlines and isotherms, respectively, while the average Nusselt number is viewed by some useful plots against different physical parameters and inclination angle.

In this thesis, the work of Basak *et al.* [40] is extended with the notion of internal heat generation or absorption parameter. The contribution of heat generation term is incorporated into energy equation. The impact of heat generation ($q^* > 0$) and heat absorption ($q^* < 0$) parameters on the flow by means of streamlines and isotherms has been observed. The average Nusselt number against the heat generation/absorption is also analyzed by Matlab plots.

Some valuable results obtained through this numerical study may be listed as follows;

- The convective forces for high Raleigh number ($Ra \geq 10^4$) enhanced inside the cavity. At high Raleigh number, an increment in the fluid flow and heat flow is observed due to the strong convection for all considered cases of q^*. Large values are noticed for the magnitude of streamfunction at the center of the cavity irrespective of the Prandtl number and inclination angle.
- At $q^* = 5$, heat transfer rate decreases for all inclination angles. For small values of q^*, the rate of heat transfer increases for lower values of ϕ and decreases at high inclination angle (i.e. $\phi = 75°$).
- Rate of heat transfer decelerates with an augmentation in the heat generation parameter ($q^* > 0$) for all cases of Ra. On the other hand, heat transfer is enhanced for the heat absorption parameter ($q^* < 0$) and attained maximum values at high Raleigh number.

5.1 Future determination

In future, the work presented in this thesis may be extend in the following direction

- Observing the magnetohydrodynamics effect on heat flow.
- Analyzing the impact of porous media.
- To perform the non-stationary simulation.
- Apply the higher order finite elements in space.
- Apply the Galerkin discretization scheme for temporal discretization.

Bibliography

[1] H. F. Oztop, Y. Varol, and A. Koca. Experimental investigation of cooling of heated circular disc using inclined circular jet. *International Communications in Heat and Mass Transfer*, 38(7):990–1001, 2010.

[2] Y. C. Pei. Thermoelastic damping in rotating flexible micro-disk. *International Journal of Mechanical Sciences*, 61:52–64, 2012.

[3] A. Muftuoglu and E. Bilgen. Heat transfer in inclined rectangular recievers for concentrated solar radiation. *International Communications in Heat and Mass Transfer*, 35(5):551–556, 2008.

[4] M. Rahimi, I. Owen, and J. Mistry. Thermal stresses in boiler tubes arises from high-speed cleaning jets. *International Journal of Mechanical Sciences*, 45:995–1009, 2003.

[5] C. Nieto, H. Power, and M. Giraldo. A boundary integral equation formulation for the thermal creep gas flow at finite Peclet numbers. *International Journal of Mechanical Sciences*, 88:267–275, 2014.

[6] A. Bahrami, D. T. Valentine, and D. K. Aidun. Computational analysis of the effect of welding parameters on energy consumption in GTA welding process. *International Journal of Mechanical Sciences*, 93:111–119, 2015.

[7] M. Turkyilmazoglu. Exact solution for the incompressible viscous magnetohydrodynamics fluid of a porous rotating disk flow with hall current. *International Journal of Mechanical Sciences*, 56:86–95, 2012.

[8] M. Turkyilmazoglu. The analytical solution of mixed convection heat transfer and fluid flow of a MHD viscoelastic fluid over a permeable stretching surface. *International Journal of Mechanical Sciences*, 77:263–268, 2013.

[9] H. Aminfar, M. Mohammadpourfard, and Y. N. Kahnamouei. Numerical study of magnetic field effects on the mixed convection of a magnetic nanofluid in a curved tube. *International Journal of Mechanical Sciences*, 7:81–90, 2014.

[10] M. S. Alam, M. A. Khatun, M. M. Rahman, and K. Vajraveluc. Effects of variable fluid properties and thermophoresis on unsteady forced convective boundary layer along a permeable stretching/shrinking wedge with variable Prandtl and Schmidt numbers. *International Journal of Mechanical Sciences*, 105:191–205, 2016.

[11] H. Aminfar, M. Mohammadpourfard, and F. Mohseni. Numerical investigation of thermocapillary and buoyancy driven convection of nanofluids in a floating zone. *International Journal of Mechanical Sciences*, 65:147–156, 2012.

[12] R. Kandasamy, I. Muhaimin, and R. Mohamad. Thermophoresis and Brownian motion effects on MHD boundary-layer flow of a nonofluid in the presense of thermal stratification due to solar radiation. *International Journal of Mechanical Sciences*, 70:146–154, 2013.

[13] M. A. Sheremet, I. Pop, and R. Nazar. Natural convection in a square cavity filled with a porous medium saturated with a nanofluid using the thermal noneequilibrium model with a Tiwari and Das nanofluid model. *International Journal of Mechanical Sciences*, 100:312–321, 2015.

[14] S. Roy and T. Basak. Finite element analysis of natural convective flows in a square cavity with non-uniformly heated walls. *International Journal of Thermal Sciences*, 52:112–126., 2012.

[15] M. November and M. W. Nasteel. Natural convection in rectangular enclosures heated from below and cooled along one side. *International Journal of Thermal Sciences*, 48:363–371, 2009.

[16] G. S. Shiralker and C. L. Tien. A numerical study of the effect of a vertical temperature difference imposed on a horizontal enclosure. *International Journal of Heat and Fluid Flow*, 28:1492–1506, 2007.

[17] M. M. Ganzoralli and L. F. Milanez. Natural convection in rectangular enclosure heated from below and symmetrically cooled from the sides. *Communications in Nonlinear Science and Numerical Simulation*, 15:1501–1510, 2010.

[18] A. C. Baytas and I. Pop. Natural convection in a trapezoidal enclosure filled with a porous medium. *International Journal of Mechanical Sciences*, 39:125–134, 2001.

[19] B. V. R. Kumar and Shalini. Free convection in a non-Darcian wavy porous enclosure. *International Journal of Engineering Science*, 41:1827–1848, 2003.

[20] K. Khanafer, B. Al-Azmi, A. Marafie, and I. Pop. Non-Darcian effects on natural convection heat transfer in a wavy porous enclosure. *International Journal of Heat and Mass Transfer*, 52:1887–1896, 2009.

[21] M. Zeng, P. Yu, F. Xu, and Q. W. Wang. Natural convection in triangular attics filled with porous medium heated from below. *Numerical Heat Transfer A-Appl*, 63:735–754, 2013.

[22] F. Wu, W. J. Zhou, G. Wang, X. X. Ma, and Y. Q. Wang. Numerical simulation of natural convection in a porous cavity with linearly temperature distribution under the local thermal non-equilibrium condition. *Numerical Heat Transfer A-Appl*, 68: 1394–1415, 2015.

[23] P. Biswal, A. Nag, and T. Basak. Analysis of thermal management during natural convection within porous tilted square cavities via heatline and entropy generation. *International Journal of Mechanical Sciences*, 51:893–911, 2012.

[24] A. K. Singh, S. Roy, and T. Basak. Analysis of Bejan's heatlines on visualization of heat flow and thermal mixing in tilted square cavities. *International Journal of Heat and Mass Transfer*, 55.

[25] C. Cianfrini, M. Corcione, and P. P. Dell'Omo. Natural convection in tilted square cavities with differentially heated opposed walls. *International Journal of Mechanical Sciences*, 44(5):441–451, 2005.

[26] E. Baez and A. Nicolas. 2D natural convection flows in tilted cavities: porous media and homogeneous fluids. *International Journal of Heat and Mass Transfer*, 49:4773–4785, 2006.

[27] A. Dalal and M. K. Das. Laminar natural convection in an inclined complicated cavity with spatially variable wall tempeature. *International Journal of Heat and Mass Transfer*, 48(18):3833–3854, 2005.

[28] S. H. Tasnim and S. Mahmud. Laminar free convection inside an inclined l-shaped enclosure. *International Communications in Heat and Mass Transfer*, 33(8):936–942, 2006.

[29] D. Z. Jeng, C. S. Yang, and C. Gau. Experimental and numerical study of transient natural convection due to mass transfer in inclined enclosure. *International Journal of Heat and Mass Transfer*, 52(1-2):181–192, 2009.

[30] H. Ozoe, H. Sayama, and S. W. Churchill. Natural convection in an inclined square channel. *International Journal of Heat and Mass Transfer*, 17:401–406, 1974.

[31] J. Rasoul and P. Prinos. Natural convection in an inclined enclosure. *International Journal of Numerical Methods for Heat and Fluid Flow*, 7:438–478, 1997.

[32] I. Catton, P. S. Ayyaswamy, and R. M. Clever. Natural convection flow in a finite rectangular slot arbitrarily oriented with respect to the gravity vector. *International Journal of Heat and Mass Transfer*, pages 173–184, 1974.

[33] F. J. Hamady, J. R. Lloyd, H. Q. Yang, and K. T. Yang. Study of local natural convection heat transfer in an inclined enclosure. *International Journal of Heat and Mass Transfer*, 32:1697–1708, 1989.

[34] K. Al-Farhny and A. Kuran. Numerical study of double diffusive natural convective heat and mass transfer in an inclined rectangular cavity filled with porous medium. *International Communications in Heat and Mass Transfer*, 39:174–181, 2012.

[35] A. J. Chamkha. Effects of heat generation/absorption and thermophoresis on hydromagnetic flow with heat and mass transfer over a flat surface. *International Journal of Numerical Methods for Heat and Fluid Flow*, 10:432–439, 2000.

[36] M. M. Molla, M. A. Hossain, and L. S. Yao. Natural convection flow along a vertical wavy surface with uniform surface temperature in the presence of heat generation/absorption. *International Journal of Thermal Sciences*, 34:157–163, 2004.

[37] M. M. Molla, M. A. Hossain, and M. C. Paul. Natural convection flow from an isothermal horizontal circular cylinder in the presence of heat generation. *International Journal of Engineering Science*, 44:949–955, 2006.

[38] T. Basak, A. K. Singh, T. P. Akshaya Sruthi, and S. Roy. Finite element simulations on heat flow visualization and entropy generation during natural convection in

inclined square cavities. *International Communication in Heat and Mass Transfer*, 51:1–8, 2014.

[39] F. M. White. Viscous fluid flow. *McGraw-Hill, Inc.*, 2, 1992.

[40] J. H. Ferziger and M. Peric. Computational methods for fluid dynamics. *Springer*, 3, 2002.

[41] R. Lohner. Applied computational fluid dynamics techniques. *Wiley*, 2, 2008.

[42] S. Hussain, F. Scheiweck, and S. Turek. Efficient Newton multigrid solution techniques for higher order space time Galerkin discretizations of incompressible flow. *Applied Numerical Mathematics*, 83:51–71, 2014.

[43] F. Kuznik, J. Vareilles, G. Rusaouen, and G. Krauss. A double-population Lattice Boltzmann method with non-uniform mesh for the simulation of natural convection in a square cavity. *International Journal of Heat and Fluid Flow*, 28:862–870, 2007.

[44] H. N. Dixit and V. Babu. Simulations of high Raleigh number natural convection in a square cavity using the Lattice Boltzmann method. *International Journal of Heat and Mass Transfer*, 49:727–739, 2006.

[45] G. D. V. Davis. Natural convection in a square cavity: a benchmark numerical solutions. *International Journal for Numerical Methods in Fluids*, 3:261–282, 2009.

[46] R. Djebali, M. E. Ganaoui, H. Sammouda, and R. Bennacer. Some benchmarks of a side wall heated cavity using Lattice Boltzmann approach. *Fluid Dynamics and Material Processing*, 83:51–71, 2014.